



Distribution and migration mechanism of fluoride in groundwater in the Manas River Basin, Northwest China

Yalei Liu^{1,2,3} · Menggui Jin^{1,2,3} · Bin Ma^{1,2,3} · Jianjun Wang^{1,2,3}

Received: 11 September 2017 / Accepted: 12 April 2018 / Published online: 27 April 2018
© Springer-Verlag GmbH Germany, part of Springer Nature 2018

Abstract

Elevated fluoride (F) concentration in groundwater is posing a public health risk in the Manas River Basin (MRB), Northwest China. Based on the characterization of regional groundwater flow, 90 groundwater samples from aquifers were analyzed, along with top-soil leachate and pore-water samples from aquitards. Stable oxygen ($\delta^{18}\text{O}$) and hydrogen isotopes, radiocarbon and hydrochemical analyses of the groundwater and pore-water samples were conducted to trace groundwater hydrological and hydrochemical processes and thereby understand the distribution and migration mechanism of F. The groundwater is recharged by meteoric precipitation through vapor condensation processes in the Tianshan Mountains. The F concentration in groundwater samples from this basin ranged from 0.11 to 48.15 mg/L (mean 2.56 mg/L). In 37 of the 90 groundwater samples, the F concentrations were above the safe level for drinking water. The F concentrations progressively increased with the residence time and well depths in the northwest of the alluvial-fluvial plain, where groundwater is overexploited for agricultural and domestic use. Positive correlations between F and sodium (Na)/calcium (Ca) indicate that the enrichment and migration of F are influenced by cation exchange processes under high-Na and alkaline pH conditions. The relationships between $\delta^{18}\text{O}$ and F and chloride (Cl) concentrations were nonlinear due to leaching and mixing processes. This shows that vertical leaching by irrigation return flow and mixing with pore water are the dominant processes driving the migration of F in the groundwater flow system of MRB, in addition to geochemical processes.

Keywords Fluoride · Aquitards · Arid regions · Stable isotopes · China

Introduction

Elevated fluoride (F) concentrations (>1.5 mg/L) have been observed in groundwater across the globe (Ali et al. 2016; Vithanage and Bhattacharya 2015), especially in arid and

semiarid areas such as Mexico (Irigoyen et al. 1995), African countries (Tekle-Haimanot et al. 2006), Pakistan (Rafique et al. 2009), India (Handa 1975; Jacks et al. 2005; Meenakshi et al. 2004; Vikas et al. 2013), and Northwest China (Amini et al. 2008; Currell et al. 2011; Guo et al. 2007, 2012; He et al. 2013; Li et al. 2015). Groundwater resources are critical for meeting domestic, industrial and agricultural water demands in such areas (Rockström et al. 2009; Williams 1999). Soluble F is commonly present as a minor element in groundwater, soils and crops. The resultant F in food and drinking water can be easily adsorbed by humans and affects physical health (Amini et al. 2008; Ayoob and Gupta 2006; Irigoyen et al. 1995). Excessive intake of F in concentrations higher than the allowable limit set by the World Health Organization (WHO; 1.5 mg/L) causes various types of fluorosis depending on the concentration and exposure time, the most commonly observed are dental and skeletal fluorosis (WHO 2004; Rango et al. 2014).

In Northwest China, more than 60 million people live in areas where the risk of fluorosis is high. More than 1 million

Published in the special issue “Groundwater sustainability in fast-developing China”

✉ Menggui Jin
mgjin@cug.edu.cn

- ¹ State Key Laboratory of Biogeology and Environmental Geology, China University of Geosciences, Wuhan 430074, People's Republic of China
- ² Laboratory of Basin Hydrology and Wetland Eco-restoration, China University of Geosciences, Wuhan 430074, People's Republic of China
- ³ School of Environmental Studies, China University of Geosciences, Wuhan 430074, People's Republic of China

people have been diagnosed with dental and skeletal fluorosis in Xinjiang province (Ministry of Health of China 2015). Elevated F concentrations in groundwater, used as drinking and irrigation water sources, are responsible for this public health problem (Li et al. 2015; Rango et al. 2014). Groundwater in the Manas River Basin (MRB), one of the most productive areas for cash crops, has elevated F concentrations (Chen et al. 2009; Luan et al. 2016). Groundwater is a major water source for domestic and agricultural use in this area, resulting in high F exposure to humans. Luan et al. (2016) investigated groundwater fluoride concentrations in Shihezi City; however, the spatial distribution and migration mechanisms of F in the groundwater in the MRB have not been systematically reported so far. Soluble F ions in groundwater can be formed due to geological factors (Gaciri and Davies 1993; Jacks et al. 2005; Nordstrom and Jenne 1977) and anthropogenic activities (Chae et al. 2007; Rafique et al. 2009). The weathering of fluorine-bearing minerals in sediments can release F into the pore water in the aquitards and the groundwater in the aquifers (Currell et al. 2011; Kwong et al. 2015); therefore, longer water residence time in sediments is believed to help increase F concentration owing to efficient water–rock interactions. The residence time of the Quaternary groundwater in this basin has been reported to range from modern to more than 10,000 years (Liu et al. 2006; Tian et al. 2010). The quality of the groundwater is also degraded due to the irrigation return flow and enrichment by soil contaminants when there is a strong evapotranspiration effect on the soils and waters in such arid and semiarid basins (Chen et al. 2009; Negrel et al. 2011; Perrin et al. 2011). Irrigation, combined with the increasing use of phosphate fertilizer and fluorine pesticides, can increase F concentrations in waters and soils (Kim et al. 2011; Rao 2003). The variations in the hydrogeochemical characteristics of groundwater such as the calcium (Ca) and bicarbonate (HCO_3) concentrations and pH conditions, also affect the F distribution and migration, through the precipitation and dissolution of F-bearing minerals (Jacks et al. 2005; Reddy et al. 2010). Therefore, local hydrological and hydrogeochemical conditions are important factors to control F concentration, distribution and migration in groundwater (He et al. 2013; Li et al. 2015).

The main objectives of this study are to: (1) investigate F abundance and spatial distribution in the groundwater of the MRB and (2) elucidate the hydrological and hydrogeochemical processes responsible for the enrichment and migration mechanisms of F in the groundwater. This study not only improves understanding of the hydrological and hydrogeochemical processes that control F concentration in groundwater but also formulates strategies for irrigation regimes and the sustainable utilization of groundwater resources to reduce the risk of F exposure.

Hydrogeological background

The MRB is an arid inland basin located in the south of the Junggar Basin in Xinjiang province in Northwest China. It covers an area of $17 \times 10^3 \text{ km}^2$ and has four major oases: Shihezi, Mosuowan, Jin'an and Xiayedi (Fig. 1). The Manas River, the largest inland river in this basin, originates by precipitation and melting of glaciers in the Tianshan Mountains. It flows through the basin area, supplies irrigation water, and reaches the terminal Manas Lake with an average flux of $1.27 \times 10^9 \text{ m}^3/\text{year}$. The influences of the westerly winds and Mongolian anticyclone result in an arid climate with hot summers and freezing winters (Bothe et al. 2012). Mean annual precipitation is 200 mm and the mean annual potential evapotranspiration rate is 1,500 mm.

The Quaternary sediments in the MRB comprise interstratified gravels, clay, and sand, and constitute a multiple aquifer/aquitard system for storing groundwater. Groundwater generally flows from the southern mountains to the northern Gurbantunggut Desert and finally into the terminal Manas Lake. However, anthropogenic activities, such as groundwater exploitation and interception by reservoirs for retaining surface water, have changed the Quaternary groundwater flow paths in the past 60 years (Chen et al. 2009); in particular, groundwater exploitation supplied 50% of the total water use in 2010. The regional groundwater levels declined 10–60 m from 1980 to 2003 and have been continuously declining since then, due to over-pumping; thus, groundwater depression cones have developed and are distributed at the margins of the desert area. As a result, the hydraulic gradients between the shallow and deep aquifers are inversed with respect to those natural conditions in some areas, where groundwater leaks from the upper shallow aquifers to deep aquifers and the inter-aquitards are consolidated to release pore water to adjacent aquifers (Huang et al. 2012; Zhou et al. 2013).

The main recharge sources for groundwater are the vertical infiltration from rivers, lateral inflow of groundwater at the mountain front, irrigation return flow, and channel leakage on the plain. The media characteristics, hydraulic gradients and the residence times shown in Fig. 2 demonstrate a decreasing groundwater velocity along the groundwater flow path. Low rainfall in this basin can hardly infiltrate into the shallow aquifers because of the intense evapotranspiration. Withdrawal of groundwater and evapotranspiration are the principle means of discharge in the inland basin (Chen et al. 2009).

Materials and methods

A total of 90 groundwater samples from MRB water supply wells in 2015 and 2016 (Fig. 1c) were collected. This included 32 groundwater samples that were collected and reported by

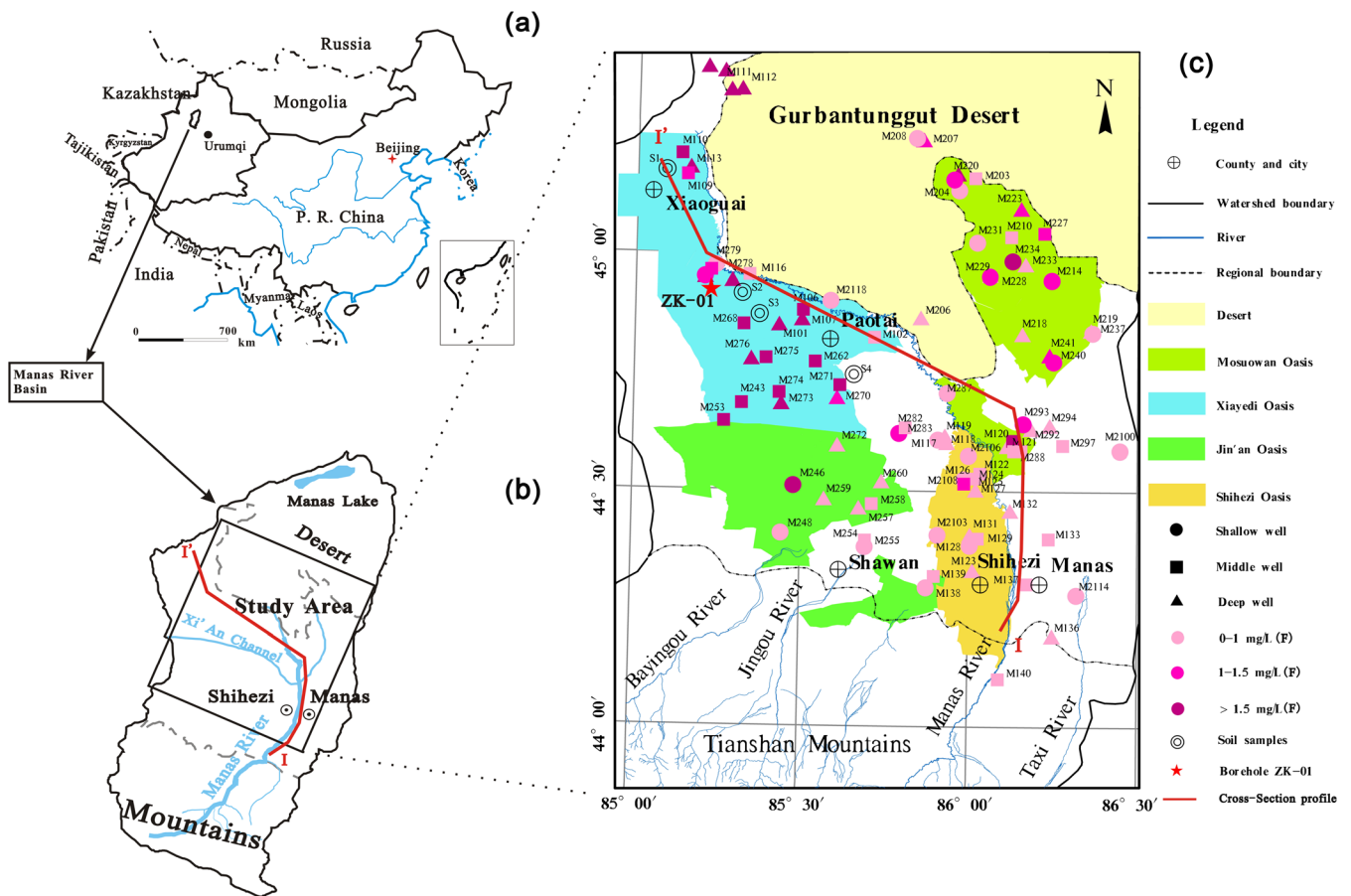


Fig. 1 Location of **a** Manas River basin in Xinjiang Province, **b** the study area and **c** sample locations with fluoride concentrations in the Manas River Basin

Ma et al. (2017), while the remaining were sampled as part of this study. Most well depths range from 10 to 450 m. From these wells, 26 samples were collected from shallow wells (depth less than 50 m), 32 samples from middle-depth wells (50–150 m) and 32 samples from deep wells (150–450 m). During the sampling periods, no significant precipitation occurred. Each well was purged for more than 10 min before sampling. Electrical conductivity (EC), pH and temperature (T) were recorded using Hach instruments (Hach 40d, USA); CO₃ and HCO₃ concentrations were determined by the titration method. All collected water samples were filtered through 0.45-μm membranes and then stored in 50-ml polyethylene bottles; furthermore, samples for cation measurements were acidized with ultra-purified HNO₃ to pH < 2 and those for anion analysis were stored directly. All samples for hydrogen and oxygen isotopes measurements were collected in polyethylene bottles and sealed with Para-film to avoid fractionations by evaporation and isotope exchange with air.

Soil samples at four sites were collected at 50-cm intervals along the profile (shown in Fig. 1c), and each sample was stored in a zip-lock bag. All soil samples were dried, grinded and sieved through a 1-mm screen for further analyses in the laboratory at room temperature. The soluble ions in soil

samples were leached by deionized water (soil:water = 1:5 by weight ratio) after shaking and centrifuge, and subsequently filtered through 0.45-μm membranes.

A borehole (ZK-01) with a depth of 103 m was drilled without fluids in August 2016 in the Xiayedi Oasis (for location see Fig. 1c). Sediment samples for particle-size analysis were collected at 0.5–2-m intervals along the borehole depth, and tested by a laser diffraction particle size analyzer (LS I3 320, Beckman Coulter, California, USA). Eight undisturbed core samples were collected from the aquitards at 10–20-m depth intervals, packed in polyethylene film and stored in a cooler box. Pore water was then extracted from the core sample by squeezing in the laboratory (Li et al. 2013; Kwong and Jiao 2016).

For all groundwater, leachates of soils and pore-water samples, cations (all acidized) were measured using inductively coupled plasma optical emission spectrometry (IRIS Intrepid II XSP, Thermo Elemental, MA and USA), and anions were analyzed by ion chromatography (Metrohm 761 Compact IC, Switzerland). Hydrogen and oxygen isotopes were measured by a Finnigan MAT-253 mass spectrometer (Thermo Fisher, USA, manufactured in Bremen, Germany) through a temperature conversion elemental analysis (TC/EA) method and

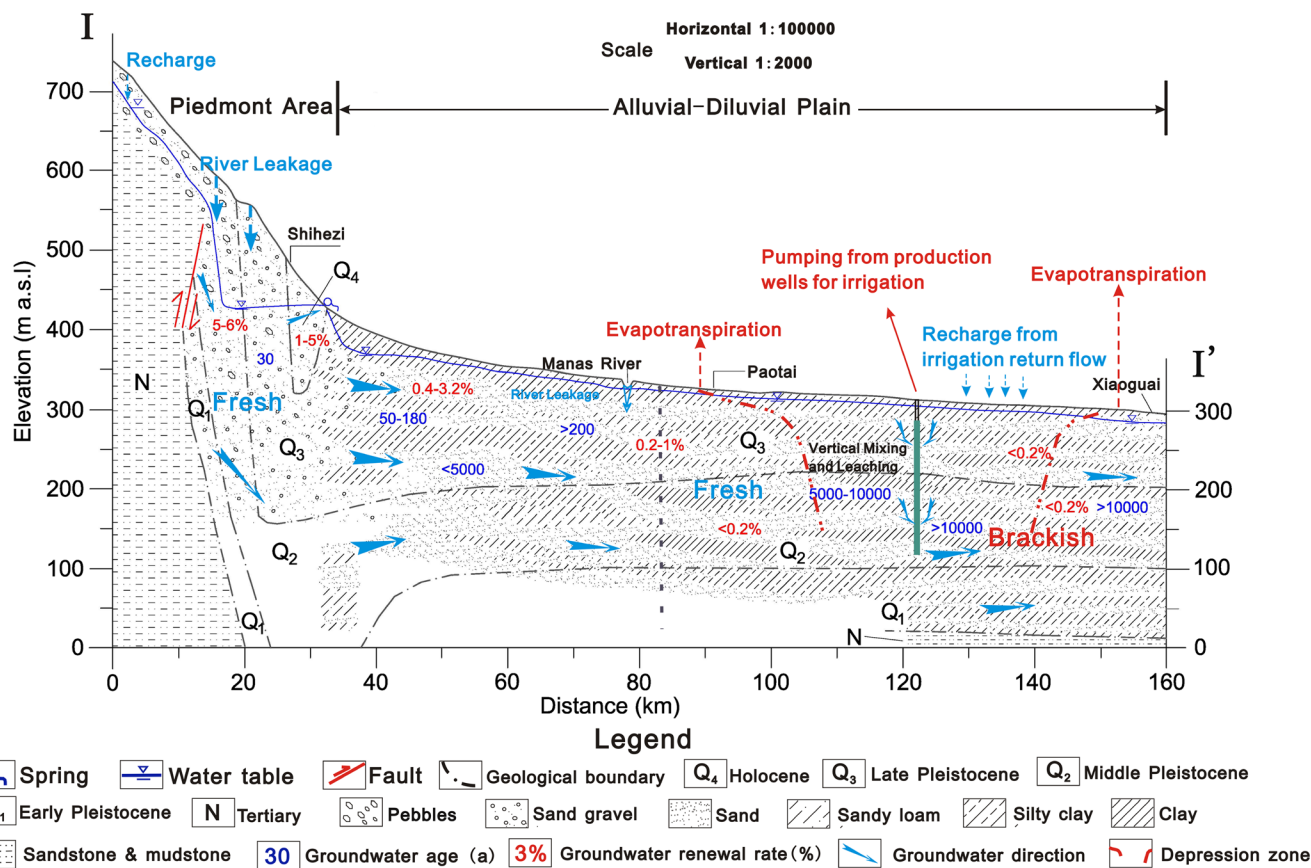


Fig. 2 Hydrogeological cross-section along the I-I' line in Fig. 1b (modified from Ma et al. 2017 and Tian et al. 2010)

normalized to the Vienna Standard Mean Ocean Water (VSMOW) standards. Instrument precisions for δD and $\delta^{18}O$ were ± 0.5 and $\pm 0.1\text{‰}$, respectively. ^{14}C contents of some groundwater samples had been measured through an ultra-low level liquid scintillation spectrometer (1220 Quantulus, PerkinElmer, USA). The hydrogeochemistry and isotope measurements were all performed at China University of Geosciences, Wuhan.

Results

Hydrogeochemistry in the Manas River Basin

Groundwater with total dissolved solids (TDS) $>1,000$ mg/L is called saline groundwater and is widely distributed in the MRB (13 out of 26 shallow groundwater samples, 13 out of 32 middle ones, and 6 out of 32 deep ones are classified as saline). A trend of increasing TDS concentration for the deep groundwater has been observed in the past few decades (Chen et al. 2009).

Groundwater pH is usually near neutral and slightly alkaline (7.3–11.2) in the MRB. Chloride (Cl) and sulfate (SO_4), and sodium (Na), are the predominant anions and cation, respectively, in the saline groundwater (TDS >1 g/L; Fig. 3).

HCO_3^- and Ca are the predominant anion and cation, respectively, in most MRB fresh groundwater samples. The HCO_3^- concentrations of groundwater samples are between 54.92 and 900.00 mg/L, Cl concentrations between 8.07 and 3,773.97 mg/L, Na concentrations between 10.6 and 4,185.95 mg/L, and Ca concentrations between 1.91 and 519.82 mg/L. The regression line of the Cl/Na ratios is approximately 0.5 (Fig. 4a, 0.52, $R^2 = 0.86$), implying that the dissolution of halite contributes to the formation of the Cl anions, in addition to the weak evapotranspiration of groundwater and mixing processes. The positive relationship between Na and SO_4 indicates that SO_4 may be balanced by Na from the dissolution of sodium sulfate (Fig. 4b). The groundwaters are generally Na•Ca- HCO_3 , Na- SO_4 and Na-Cl types in the MRB, from the recharge area to discharge area.

Groundwater hydrogen (δD) and oxygen ($\delta^{18}O$) isotope values range from -27.21 to -114.94‰ and -4.24 to -12.72‰ , respectively. The $\delta^{18}O$ vs. δD diagram in Fig. 5 shows that most groundwater samples locate along the local meteoric water line (LMWL) of Urumqi (about 150 km east of the study area, data from the International Atomic Energy Agency/World Meteorological Organization 2002). The groundwater regression line (GWL) slope is 6.68 ($R^2 = 0.85$; Fig. 5), lower than the slope of the LMWL (7.23). Most samples are distributed to the left of the global meteoric water line

Fig. 3 Piper diagram of groundwater hydrogeochemical characteristics in the MRB

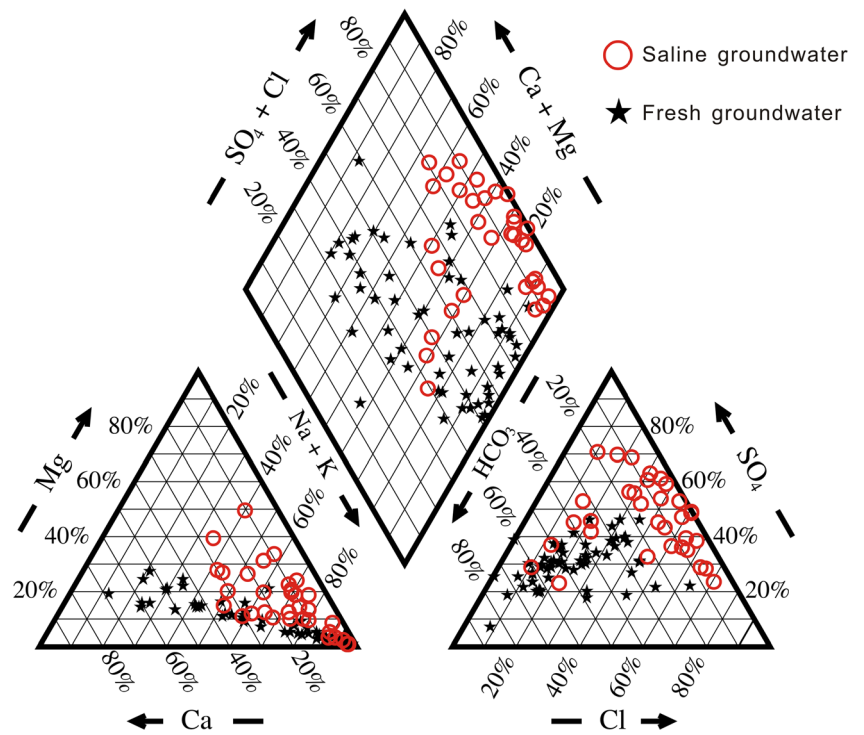


Fig. 4 Plots of **a** Na vs Cl and **b** Na vs SO_4 concentrations in the groundwater samples, indicating that dissolution of halite and mirabilite partially contributes to the Na concentrations

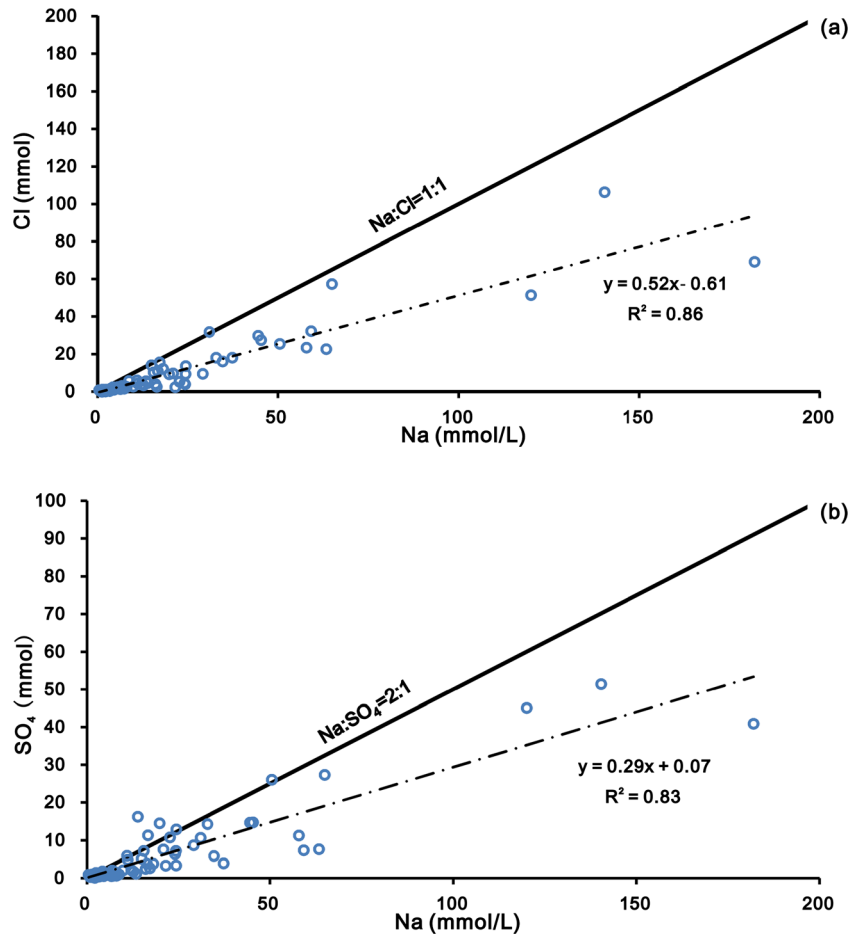
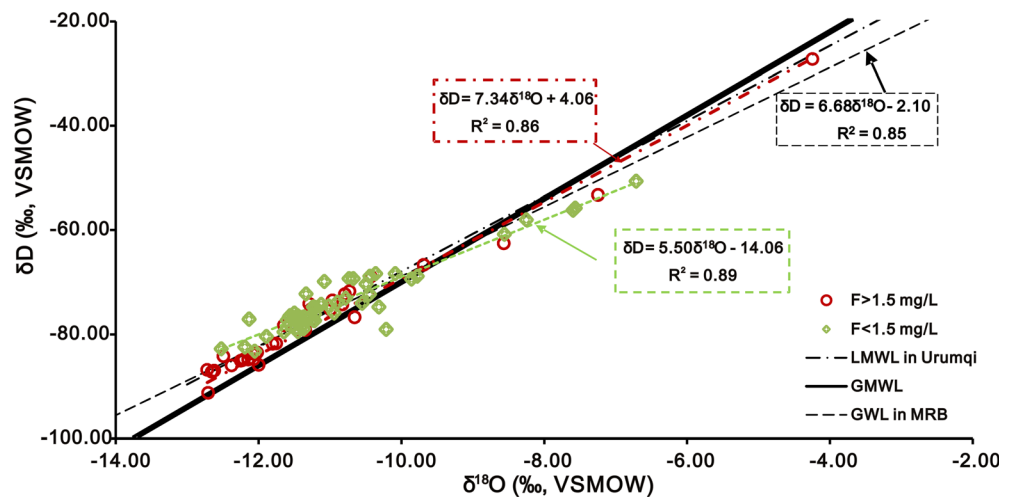


Fig. 5 Relationship between δD and $\delta^{18}O$ of groundwater samples in the MRB. Most samples distribute on or nearly parallel with the local meteoric water line (LMWL, 7.23) in Urumqi, particularly the elevated-F groundwater



(GMWL). This shows that the groundwater is mainly formed by meteoric precipitation through condensation of the evaporated water in the mountains and slightly affected by the evaporation around the MRB (Pang et al. 2017).

Hydrogeochemical and isotopic characteristics of the groundwater in the shallow, middle, and deep wells are presented in Table 1. The temperature (T) of groundwater samples increases from the shallow to the deep wells, whereas the mean and median salinity, HCO_3^- , Ca, Mg, δD and $\delta^{18}O$ show decreasing trends with well depth. Ca concentrations are low in the deep groundwater with high F concentrations.

Furthermore, 39.4% of all samples, especially those from the shallow wells, have elevated nitrate (NO_3^-) concentrations (>10 mg/L, WHO standard). The mean NO_3^- values also show a decreasing trend with increasing well depth. The Pearson's correlation matrix (Table 2) shows that Na and Na/Ca are significantly correlated with the F concentrations ($p < 0.05$), then following with Ca and depth. Percent modern carbon (pMC) values of ^{14}C in some groundwater samples vary from 23.5 to 86.9% (Table 3), with corresponding apparent ages increasing from 1.16 to 11.96 ka before present (BP). The adjacent samples M127 and M132, with nearly the same

Table 1 Statistical summary of the hydrogeochemical characteristics of groundwater in Manas River Basin

Parameter	Shallow groundwater				Middle groundwater				Deep groundwater			
	Max	Min	Mean	Median	Max	Min	Mean	Median	Max	Min	Mean	Median
pH	11.20	7.85	9.01	8.79	10.85	7.76	9.29	9.16	11.30	8.36	9.76	9.53
EC (ms/cm)	14.81	0.21	2.35	1.19	19.20	0.28	2.46	0.67	11.79	0.22	1.36	0.44
T (°C)	19.90	12.70	14.12	13.60	18.50	11.50	14.61	14.30	19.50	14.40	16.40	15.85
F (mg/L)	3.30	0.20	1.27	0.87	48.15	0.11	2.25 ^a	1.16	11.38	0.27	2.49	1.02
Ca (mg/L)	319.82	1.91	96.41	71.39	519.82	6.06	94.97	46.53	441.15	2.26	36.20	17.09
Na (mg/L)	2,761.50	18.32	409.85	241.39	4,185.95	10.60	458.12	124.59	3,228.58	19.77	327.39	104.02
Mg (mg/L)	313.97	0.74	75.19	38.80	586.53	1.48	52.39	12.12	225.84	0.44	13.46	3.95
Cl (mg/L)	1,822.87	8.07	251.93	90.28	2,455.18	10.03	379.28	80.20	3,773.97	6.66	273.69	39.53
SO_4 (mg/L)	4,326.93	24.53	598.67	177.47	3,922.82	32.44	599.64	113.00	4,933.00	7.97	299.36	64.46
NO_3^- (mg/L)	78.53	0.00	18.55	5.12	85.75	0.00	7.89	3.89	16.45	0.00	4.28	0.98
HCO_3^- (mg/L)	900.00	72.61	331.59	327.36	838.99	54.92	178.58	128.41	247.05	70.17	117.23	100.36
Salinity (mg/L)	9,793.13	178.68	1,786.46	993.79	11,905.21	180.16	1,736.10	518.53	12,688.08	140.16	1,055.10	289.94
δD (‰)	-50.67	-79.47	-71.09	-73.88	-27.21	-114.94	-75.36	-76.48	-68.90	-86.99	-78.74	-78.08
$\delta^{18}O$ (‰)	-6.71	-12.13	-10.27	-10.76	-4.24	-12.72	-10.90	-11.22	-10.32	-12.62	-11.59	-11.55
SI_{halite}	-4.06	-8.28	-6.35	-6.19	-3.76	-8.14	-6.21	-6.36	-3.69	-8.05	-6.67	-6.96
$SI_{fluorite}$	0.12	-2.25	-1.43	-1.58	2.11	-3.00	-1.10	-1.22	1.09	-2.59	-1.38	-1.69
$SI_{calcite}$	0.69	-0.81	0.09	0.16	1.54	-0.84	0.06	0.08	0.97	-0.97	0.29	0.44
$SI_{dolomite}$	1.11	-2.04	0.20	0.36	3.15	-2.02	-0.04	0.43	2.07	-2.29	0.21	0.52

^a The maximum 48.1 mg/L has not been included because it is considered abnormal

Table 2 The Pearson's correlation matrix for analyzed parameter significance on the F concentrations ($n = 89$)

	F	Ca	K	Na	Mg	Cl	SO ₄	NO ₃	HCO ₃	Na/Ca	Depth	pH	EC
F	1												
Ca	0.153	1											
K	0.027	0.435**	1										
Na	0.284**	0.765**	0.389**	1									
Mg	0.064	0.811**	0.13	0.770**	1								
Cl	0.331**	0.798**	0.398**	0.925**	0.690**	1							
SO ₄	0.265**	0.885**	0.517**	0.912**	0.764**	0.915**	1						
NO ₃	0.031	0.287**	0.038	0.148	0.395**	0.193*	0.210*	1					
HCO ₃	-0.11	0.241*	0.138	0.196*	0.436**	0.059	0.216*	0.559**	1				
Na/Ca	0.211*	-0.274**	-0.187*	0.047	-0.174	-0.015	-0.102	-0.163	-0.034	1			
Depth	0.146	-0.318**	-0.112	-0.122	-0.329**	-0.073	-0.213*	-0.259*	-0.423**	0.132	1		
pH	0.057	-0.264*	-0.394**	-0.167	-0.243*	-0.102	-0.203	-0.286**	-0.445**	0.283**	0.333**	1	
EC	0.246*	0.849**	0.422**	0.960**	0.844**	0.895**	0.940**	0.216*	0.247*	-0.053	-0.201	-0.195	1

* significant at $p < 0.05$ level; ** significant at $p < 0.01$ level

depths (260 and 280 m), show different pMC values, 53.2 and 86.9%, respectively. The relative high pMC of M132 could be attributed to mixing with younger recharge water, as it is closer to Manas River.

Distribution of elevated fluoride concentrations in groundwater

In this basin area, F concentrations in groundwater range from 0.11 to 48.15 mg/L (mean of 2.05 mg/L, excluding the highest value 48.15 mg/L), of which 41.1% are higher than the WHO standard for drinking water (1.5 mg/L) and 51.1% higher than the Chinese standard (1 mg/L). The F concentrations increase systematically from the south piedmont to the northwest of the

alluvial-diluvial plain. Groundwater F concentrations are less than 1 mg/L for most wells in the Shihezi Oasis, the piedmont along the Manas River (Fig. 1c). Groundwater flow velocity and renewal rate calculated based on the ³H concentrations—determined using the methodology proposed by Salle et al. (2001)—decrease along the groundwater flow path depicted in Fig. 2 (Tian et al. 2010). Therefore, F concentrations increase due to the water–rock interactions over a prolonged residence time, potentially exceeding the safe level for drinking in the alluvial-fluvial plains, where the topography is generally flat and the deposits of fine sand and silty clay have low permeability. High F concentrations are predominantly found in groundwater along the marginal area between the alluvial-fluvial plain and the desert land. In summary, according to the contour maps

Table 3 Apparent ages of groundwater samples calculated by the ¹⁴C content (using mass spectrometry)

Sample No.	pMC	¹⁴ C apparent age (ka BP)	Depth (m)	F (mg/L)
M101	41.9 ± 1.6	7.19 ± 0.27	347	5.97
M102	69.8 ± 2.5	2.97 ± 0.11	90	0.60
M108	75.1 ± 2.7	2.37 ± 0.08	220	8.10
M109	47.9 ± 1.8	6.08 ± 0.23	120	2.12
M111	56.0 ± 2.1	4.79 ± 0.18	300	5.28
M113	64.7 ± 2.3	3.60 ± 0.13	200	4.04
M119	23.5 ± 0.9	11.96 ± 0.47	190	0.50
M120	54.6 ± 2.0	5.00 ± 0.19	300	0.90
M121	84.9 ± 3.0	1.35 ± 0.05	150	48.15
M123	43.4 ± 1.6	6.89 ± 0.26	180	0.32
M127	53.2 ± 2.0	5.22 ± 0.19	280	0.61
M131	46.8 ± 1.8	6.27 ± 0.24	350	0.48
M132	86.9 ± 3.0	1.16 ± 0.04	260	0.27
M-II	79.6 ± 0.3	1.83 ± 0.03	72	2.23
M-III	75.4 ± 0.2	2.27 ± 0.03	114	1.70

of F concentration (Fig. 6), the shallow groundwater regions with elevated F concentrations (>1.5 mg/L) are distributed in the northern and western parts (the Xiayedi and Jin'an oases) and northeastern part (the Mosuwuan Oasis) of the MRB. As to the middle and deep groundwater, the F concentrations in the northwestern part are slightly elevated, and higher than those in the southern and eastern parts (i.e., the Shihezi and Mosuwuan oases). On the basin scale, the distribution of elevated F in the shallow groundwater are consistently associated with the arable

land, where channel and river water are scarce and groundwater is highly exploited for irrigation (Fig. 1c).

Vertically, groundwater F concentrations >1.5 mg/L are distributed in the shallow, middle, and deep wells. Figure 7 shows that the F concentrations increase with well depth in the Xiayedi Oasis; however, most groundwater samples in the Shihezi Oasis have low F concentrations (<1 mg/L, Chinese standard) that are not related to well depth, because the Manas River water, with low F concentration of 0.13 mg/L, is intercepted and recharged

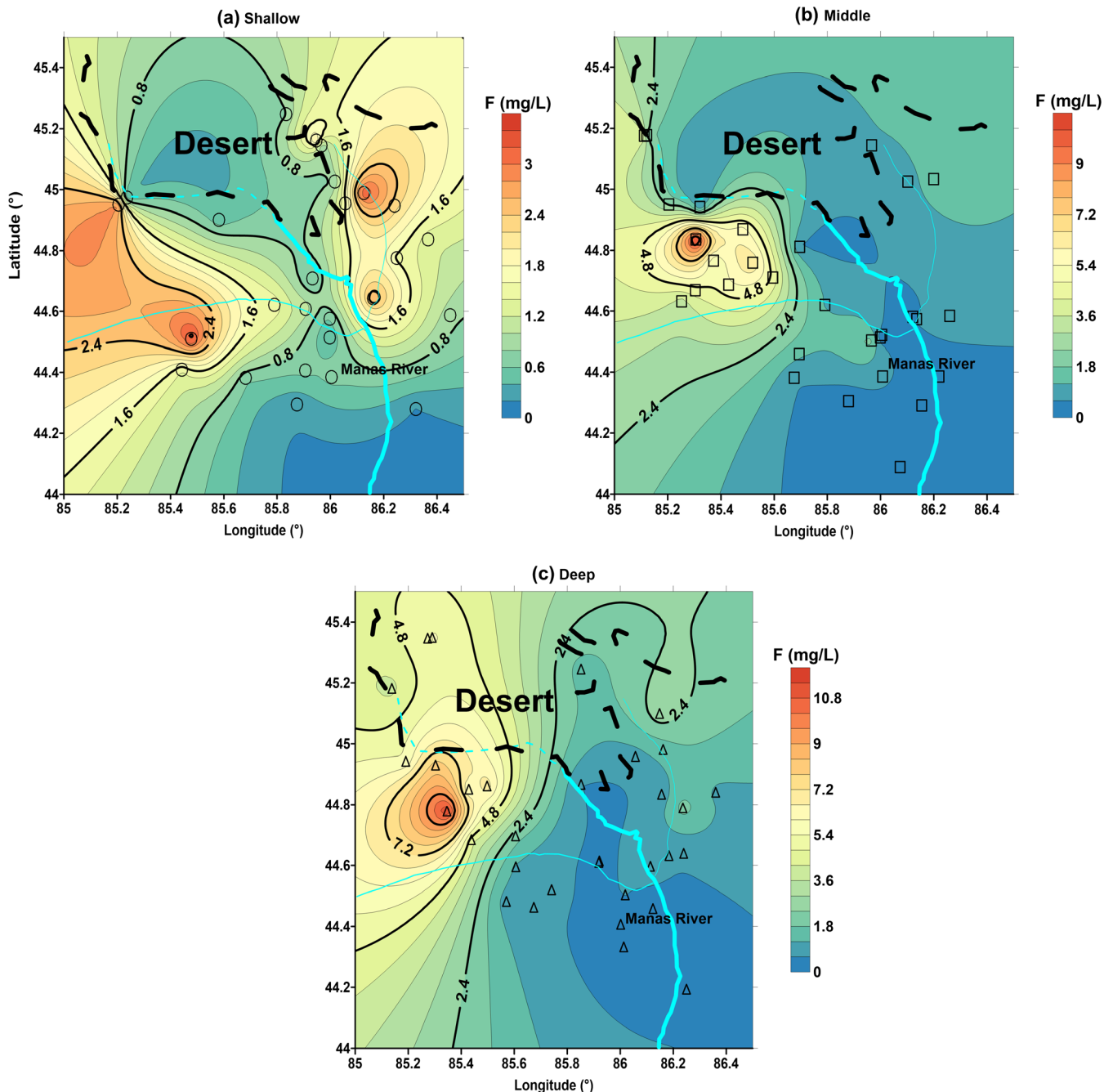


Fig. 6 Contour maps of fluoride concentrations in groundwater in the study area interpolated using the Kriging method: **a** Shallow (0–3.4 mg/L), **b** Middle (0–10.5 mg/L), and **c** Deep (0–11.5 mg/L) groundwater.

Most elevated-F groundwater samples are distributed in the mid-west and north part of Manas River Basin

into groundwater in this area. In the Mosuowan Oasis, the F concentrations in the shallow wells range from 0.85 to 3.2 mg/L, with a mean value of 1.68 mg/L; however, the concentrations range from 0.62 to 2.77 mg/L in the middle and deep wells, with a mean value of 1.20 mg/L (15 samples). Elevated F concentrations are observed in most groundwater samples from the shallow to the deep wells in the Xiayedi Oasis (Fig. 7). In this oasis, three groundwater samples associated with water levels for different aquifers from a multilevel wells cluster (ZK-01) were tested: F concentration is 2.82 mg/L for the M-I aquifer (depth 14–20 m) with a water level depth of 4.28 m, 2.23 mg/L for the M-II aquifer (60–72 m) with a water level depth of 2.84 m, and 1.70 mg/L for the M-III aquifer (100–124 m) with a water level depth of 53.1 m (Fig. 8). A downward vertical hydraulic gradient is calculated as -1.8 between the M-II and M-III aquifers in this discharging area; nonetheless, F concentrations >4 mg/L in groundwater samples mostly occur in the middle and deep wells.

Fluoride concentrations of the pore water in aquitards

Pore water in aquitards, an important component of groundwater, can release into adjacent aquifers and influence the

hydrogeochemical characteristics of the aquifer groundwater when the aquifers are highly exploited (Ortega-Guerrero et al. 1993). Elevated F concentrations are observed in the pore water along the borehole ZK-01 profile. The F concentrations in pore-water range from 3.92 to 14.04 mg/L when the samples are from depths 41.5 to 100 m (Fig. 8). F concentrations in the groundwater are far lower than those in the pore water of adjacent aquitards, but the groundwater $\delta^{18}\text{O}$ values in aquifers are more positive than those in pore water. This can be attributed to the different migration mechanisms in the aquifer and aquitards. It indicates that the migration of chemicals in pore water may be diffusion-dominated in the aquitards due to the hydrogeochemical gradients (Hendry et al. 2004; Hendry and Wassenaar 2011). Below 20 m in the profile, the nearly stable $\delta^{18}\text{O}$ values close to -13.8‰ in the precipitating vapor (Wang et al. 2016) indicate that there are no intense evaporation effects. Therefore, the elevated F concentrations in the pore water are believed to mainly originate from the dissolution of fluorite and prolonged water–rock interactions with abundant clay and silt contents, due to the migration mechanism involving diffusion over a long residence time (Kwong et al. 2015; Misra and Mishra 2007).

Fluoride abundance in soils

Leachates of the saline soils near the marginal area between the alluvial-fluvial plain and desert were extracted using deionized water for analyzing the soluble F content (Table 4). Total soluble F ranged from 99.9 to 1,390.75 mg/kg, with a median of 388.5 mg/kg, which is slightly higher than the global soil mean value of 320 mg/kg (Wenzel and Blum 1992). The major ions (Cl, Ca, Mg, and NO_3) accumulated at the surface (0–10 cm), mostly due to the intense evaporation effect in this arid basin. The decreasing Ca/Na ratios also suggest that the evaporation effect causes evaporite minerals to precipitate at the surface; however, there is a weak positive relationship between the F content and soil depth, in contrast to the Ca contents in the vadose zone as shown in Fig. 9. Elevated F concentration commonly coexists with a low concentration of soluble Ca due to the low solubility of CaF_2 and the relatively high Na contents in deeper soil.

Discussion

Correlations between the major ions and F concentrations in groundwater, along with the hydrogeochemical characteristics of pore water in aquitards and soil leachates, could provide a deeper understanding of the spatial distribution and migration mechanisms of F in the MRB.

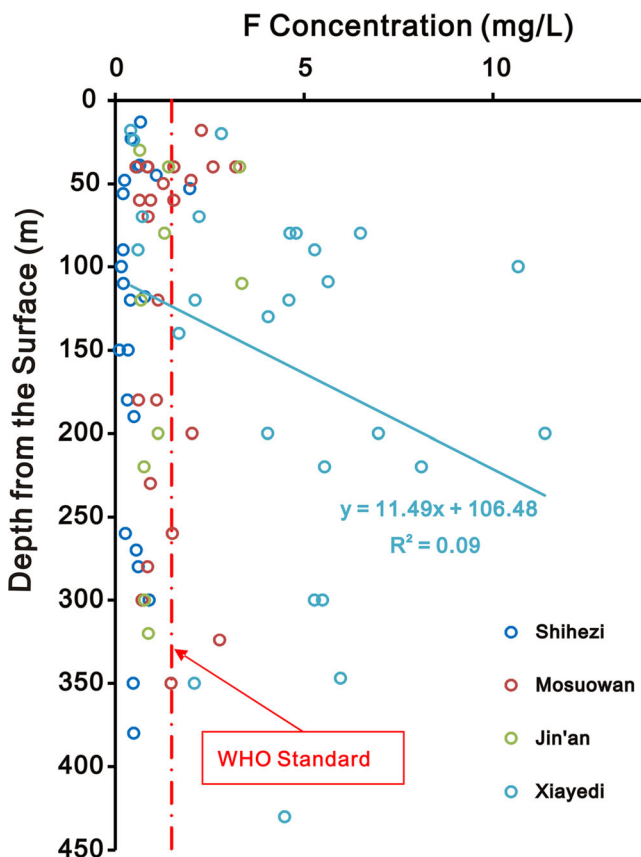


Fig. 7 Fluoride concentrations against well depths for the groundwater samples. It shows that the highest-fluoride groundwater is found in the middle and deep wells

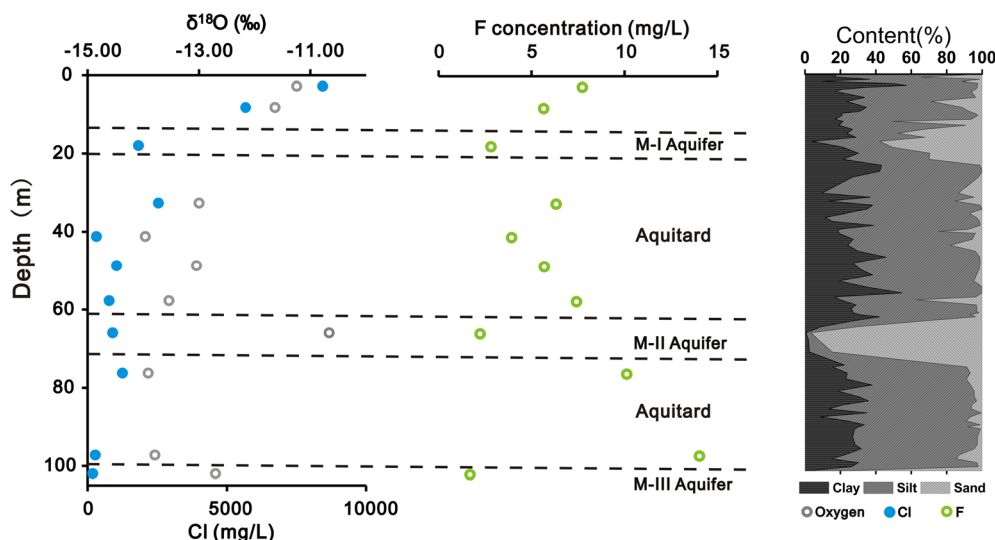


Fig. 8 $\delta^{18}\text{O}$, Cl and F concentration profiles of groundwater in aquifers and pore water in the aquitards of bore ZK-01 in the Xiayedi Oasis. The F concentrations show an increasing trend, while the $\delta^{18}\text{O}$ and Cl concentrations are nearly stable with depth >20 m from the surface, which

indicates that the pore waters are nearly independent of evaporation effects and the chemical migration mechanism is a diffusion process, deduced from the characteristics of advective groundwater flow in aquifers (Hendry and Wassenaar 2011; Kuang et al. 2016)

Development of elevated fluoride concentrations in groundwater

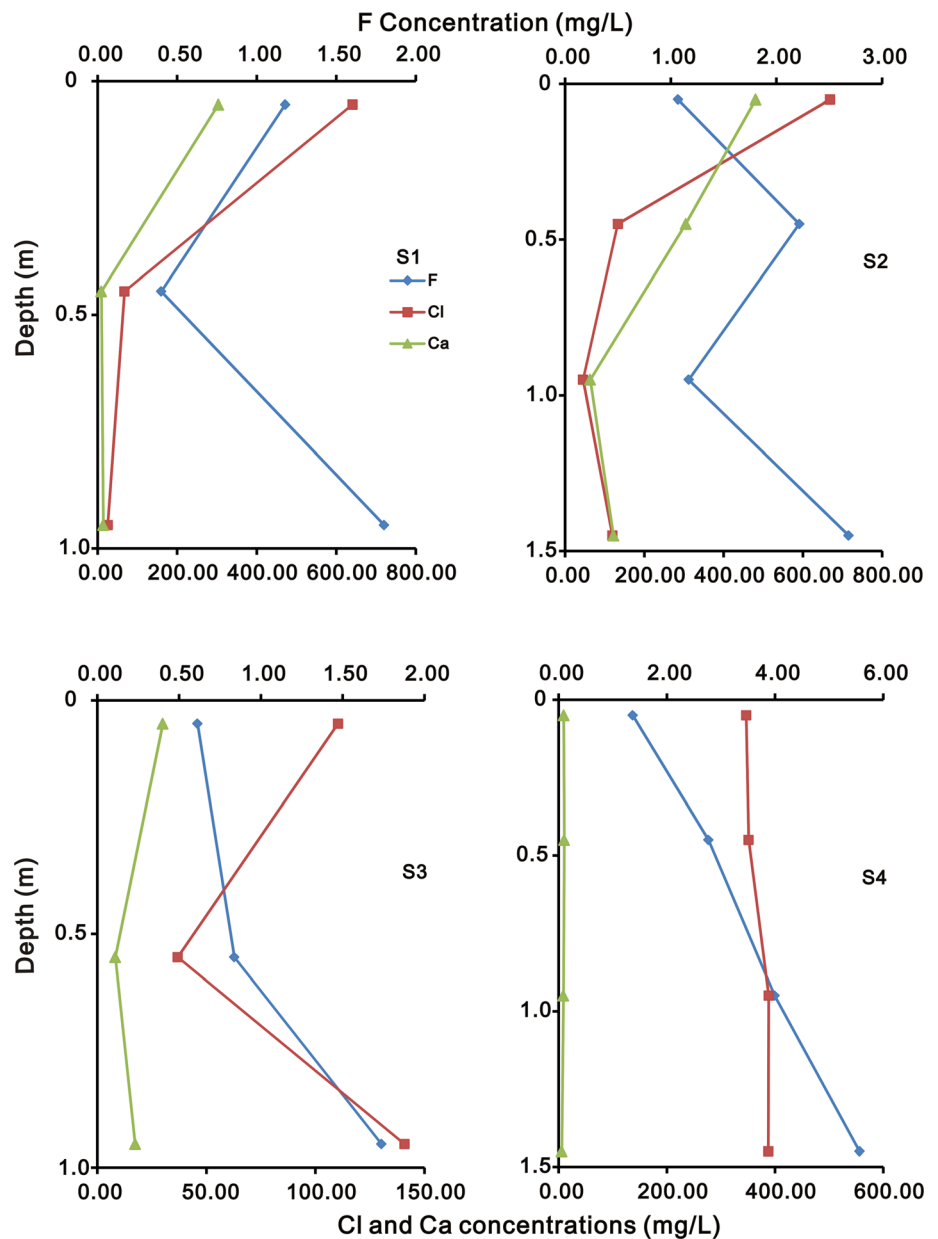
Elevated F concentrations exist in both saline and fresh groundwater samples in the MRB (Fig. 10a). High TDS (>1 g/L) coexisting with elevated F concentrations (>1.5 mg/L) is mainly observed in shallow and middle groundwater, whereas most samples with low TDS (<1 g/L)

and elevated F concentrations are from deep wells. It indicates complex sources and migration mechanisms of F in aquifers at different depths. Hydrogeochemical and hydrological processes are responsible for the increases in the F concentrations and migration in groundwater. Groundwater with elevated F concentrations generally has low Ca and high Na concentrations and high Na/Ca ratios (Fig. 10b,c); this is similar to the findings of previous studies in arid and semiarid areas (Jacks

Table 4 Hydrogeochemical characteristics of leachates of soils in the vadose zone near the margin between the alluvial-fluvial plain and desert plain. (soil:diluted water = 1:5 by weight)

Sample No.	Depth (cm)	Major ions in leachate (mg/L)									F in soil (mg/kg)
		F	Cl	NO ₃	SO ₄	Ca	Na	K	Mg	Ca/Na	
S1	0–10	1.18	641.06	58.01	631.32	303.45	215.60	2.62	48.27	1.41	294.88
	40–50	0.40	67.26	7.83	309.82	9.09	204.60	3.54	1.90	0.04	99.93
	90–100	1.80	25.27	8.50	219.46	13.98	126.80	2.35	1.62	0.11	450.38
S2	0–10	1.07	668.87	349.13	1,276.81	481.00	335.30	18.12	49.56	1.43	267.00
	40–50	2.22	133.12	47.71	1,417.57	304.60	218.05	2.65	48.18	1.40	554.00
	90–100	1.17	45.43	17.60	407.00	63.37	139.70	2.06	11.71	0.45	292.48
S3	0–10	0.61	110.39	28.42	86.21	30.09	70.14	5.00	6.52	0.43	153.18
	50–60	0.84	36.90	2.03	52.98	8.27	45.83	2.22	3.62	0.18	209.48
	90–100	1.74	140.82	8.97	110.47	17.42	141.20	2.34	8.44	0.12	434.30
S4	0–10	1.37	346.70	10.78	167.33	9.28	133.55	0.53	0.86	0.07	342.75
	40–50	2.77	351.30	3.17	394.13	10.35	528.50	1.99	7.09	0.02	692.50
	90–100	3.99	388.42	3.03	677.93	8.80	556.50	2.44	2.02	0.02	998.38
140–150	5.56	387.57	4.02	507.23	5.70	574.40	2.06	4.23	0.01	1390.75	
Mean		1.96	247.31	40.32	479.69	99.10	246.36	3.56	14.68	0.46	489.34

Fig. 9 Variations of the Cl, Ca and F concentrations in the leachates of saline soil (soil:deionized water = 1:5 by weight) vs depth from the surface in the alluvial-fluvial plain in Manas River Basin. High F concentrations always coexist with the low Ca concentrations in deep soil samples in all profiles



et al. 2005; Rafique et al. 2009; Vithanage and Bhattacharya 2015). In this study, elevated F concentrations show a weak, positive linear relationship with HCO_3 in the shallow and deep wells but negative in middle wells (Fig. 10d); this contradiction and low R^2 indicate that F ions may be derived from other sources such as fluoride-bearing fertilizers and mixing with elevated fluoride sources in addition to the geochemical processes (Currell et al. 2011; Guo et al. 2007; Li et al. 2015; Su et al. 2015). However, the high HCO_3/Ca ratios >1 (Fig. 10e) in most groundwater samples with elevated F concentrations demonstrate the competing effect of HCO_3 on the dissolution of fluorine minerals. Meanwhile, most groundwater samples with elevated F concentrations are calcite saturated ($\text{SI}_{\text{calcite}}$ value from -0.97 to $+1.54$ with

a mean value $+0.15$) which helps remove Ca from groundwater, and F concentrations show a roughly positive relationship with the $\text{SI}_{\text{calcite}}$. In all, 80 out of the 90 groundwater samples are undersaturated with respect to the fluorite ($\text{SI}_{\text{fluorite}}$ from -3 to $+2.11$, mean value -1.29), and the $\text{SI}_{\text{fluorite}}$ values increase with the F concentrations (Fig. 11). Accordingly, these imply that fluorite dissolution contributes to the F concentrations and the high F concentration might be enhanced by calcite precipitation processes (Su et al. 2015); however, some groundwater samples with elevated F concentrations are oversaturated with respect to fluorite but undersaturated with respect to calcite, as shown in group A in Fig. 11, indicating that anthropogenic activities possibly affect F enrichment.

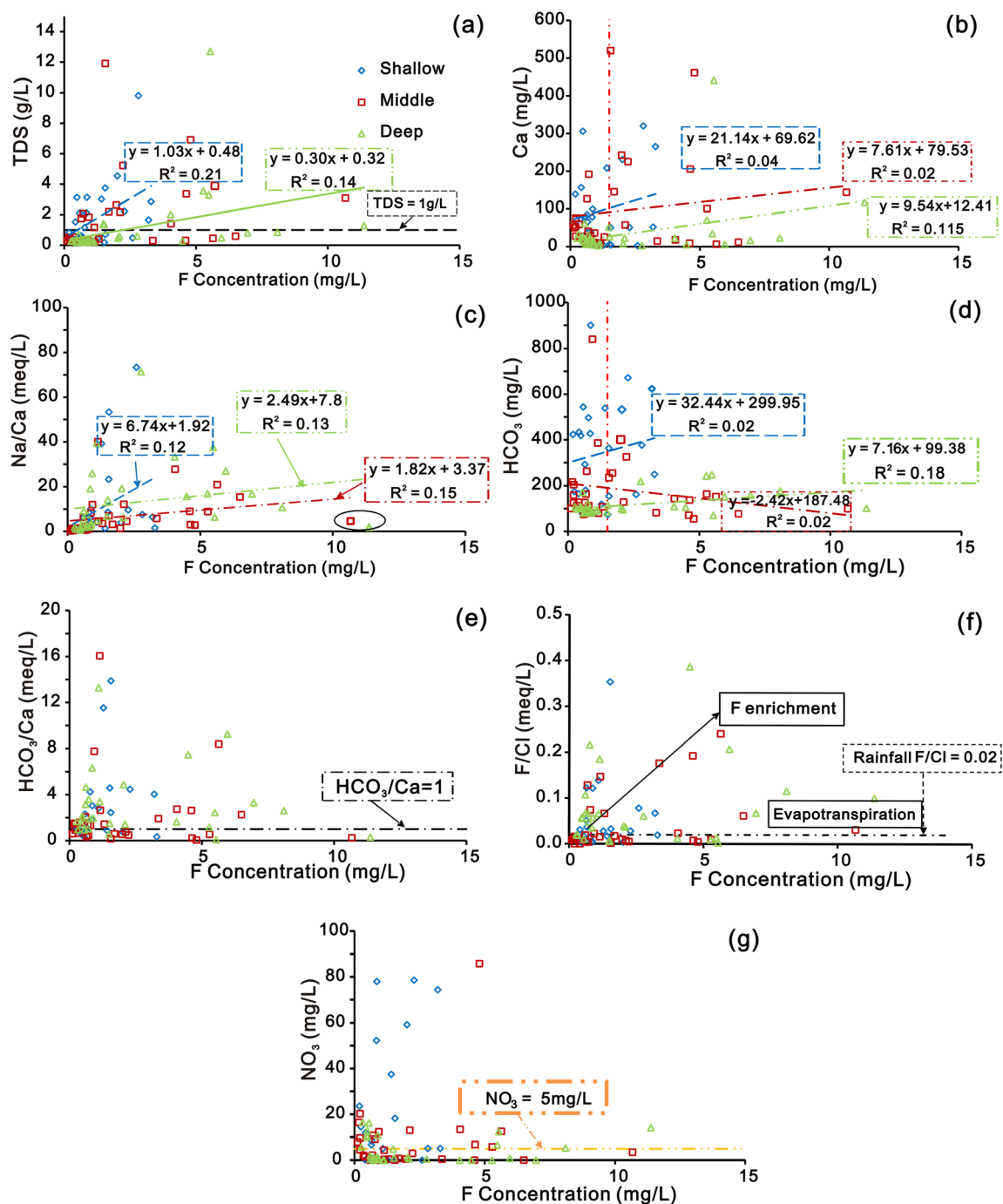


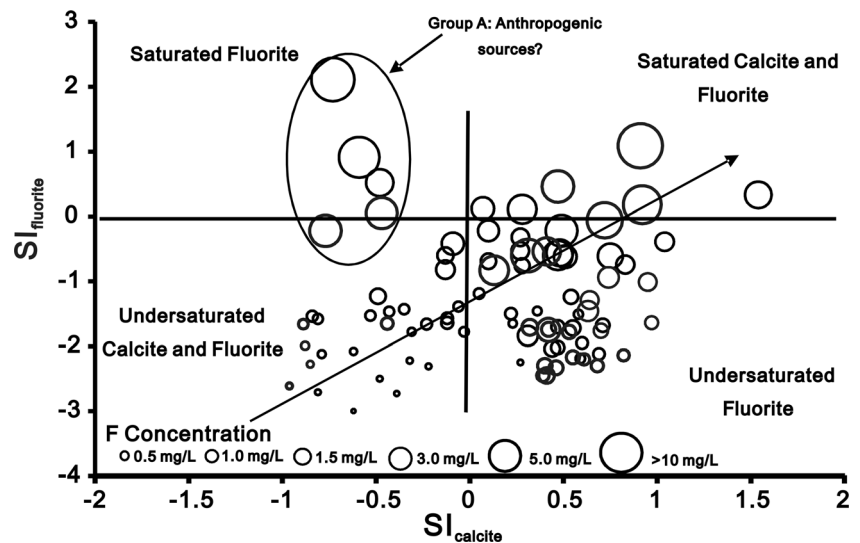
Fig. 10 Correlations between the F concentrations and salinity, Ca, Na/Ca (meq/L), HCO_3^- , HCO_3^-/Ca (meq/L), F/Cl (meq/L) and NO_3^- for groundwater in shallow, middle and deep wells. Most elevated-F groundwaters have higher Na/Ca ratios than 1, and the presence of high NO_3^-

concentrations in some elevated-F groundwater indicates that agricultural activities may affect the groundwater hydrochemistry and F concentrations and migration

The oxygen and hydrogen isotopic compositions of groundwater with elevated F concentrations show a regression line slope of 7.34 ($R^2 = 0.86$); however, for the groundwater samples with low F concentrations, the regression line slope is only 5.50 ($R^2 = 0.89$), owing to the evaporation effects (Fig. 5). Most groundwater samples have similar $\delta^{18}\text{O}$ and δD composition characteristics in both the low and elevated F

groundwater samples and the $\delta^{18}\text{O}$ values are between -12 and -10‰ . Most elevated-F groundwater is distributed to the left of the GMWL due to the origins of precipitation through vapor condensation processes in Tianshan Mountains, which are independent of evaporation effects. Some low-F groundwater distributes to the right of the LMWL and the regression line has a low slope, revealing that the evaporation effect

Fig. 11 Plot of the groundwater calcite saturation index (SI) against the fluorite saturation index (SI) against the fluorite saturation index, with fluoride concentrations indicated by the bubbles. F shows a roughly increasing trend with SI_{calcite} , indicating that oversaturation of calcite could promote dissolution of fluorite, except for group A

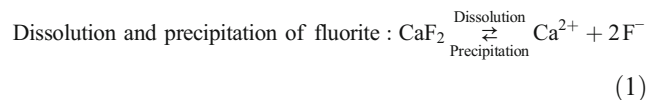


could slightly increase F enrichment in groundwater. Furthermore, the existence of low F/Cl ratios (≤ 0.02) indicates the influence of evaporation effects on the groundwater in most middle wells (Fig. 10f).

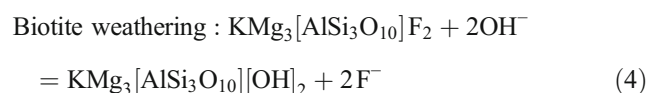
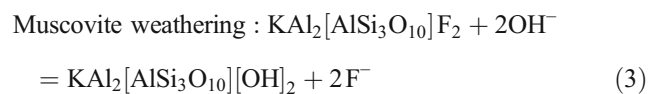
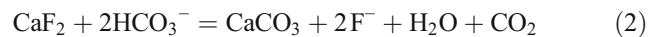
Source and migration of fluoride in groundwater

The high prevalence of elevated F concentrations in groundwater with varying residence time at all depths suggests that comprehensive geochemical and other processes influence the enrichment and migration of F in the groundwater in the MRB (e.g., sample M121 with a F concentration of 48.15 mg/L in Table 3). Soluble F ions can be formed by the dissolution of fluorite (CaF_2) and weathering of hydroxyl minerals such as biotite and muscovite in aquifers (Guo et al. 2007; Jacks et al. 2005). In the MRB, the natural groundwater flow path has changed due to groundwater overexploitation; thus, the distribution of F concentration varies spatially, corresponding to the different groundwater residence times, as illustrated by the relationship between the F concentrations and ^{14}C apparent ages (Table 3; Fig. 12). In the Shihezi Oasis, groundwater apparent age shows great variance from 1.16 to 6.89 ka BP, and all samples have low F concentrations owing to the low fluorite content in the gravels and coarse sand as well as the dilution by the Manas River. Thus, it shows low correlation between F concentrations ($R^2 = 0.13$) and ^{14}C apparent ages. Some deep groundwater samples in Xiayedi (e.g. M113 with 3.60 ka BP) are apparently younger than those in the Shihezi Oasis (e.g. M123 with 6.89 ka BP); however, the F concentrations are elevated. It indicates that the groundwater mixed with younger water, such as the irrigation return flow and the leakage from upper shallow aquifers. In the Xiayedi Oasis, groundwater F concentrations generally increase ($R^2 = 0.71$) with increasing residence time, indicating that efficient dissolution of fluorine minerals and the weathering of

hydroxyl minerals partially contribute to the increase in the F content during the groundwater migration process.

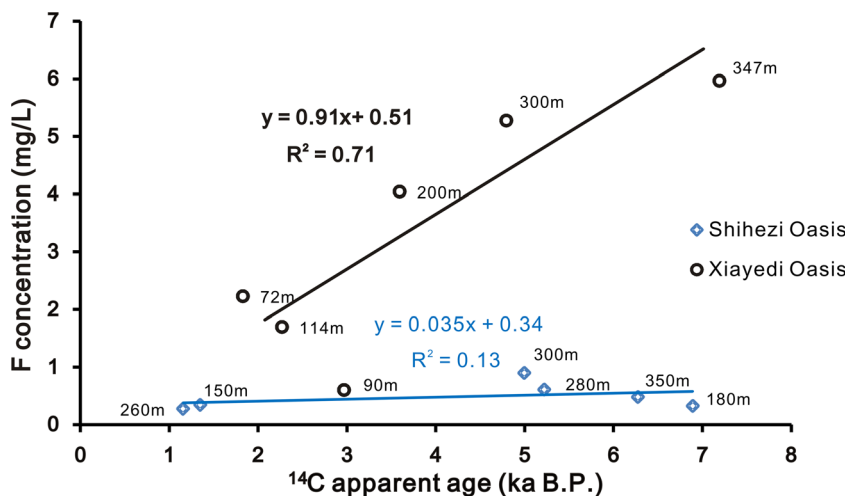


Fluorite release F during weathering of the F-bearing minerals and precipitation of calcite:



F/Cl ratios in the middle and deep groundwater are higher than those in the unpolluted rainfall (0.02; Saether et al. 1995) or the Manas River (0.03), and the relationship between F/Cl ratios and F concentrations indicate that the increase in F is influenced not only by evapotranspiration but also by the water–rock interactions (Currell et al. 2011). The sediments of the aquifers and aquitards could react with the groundwater and pore water, providing sources of soluble F ions (Currell et al. 2011; Ortega-Guerrero et al. 1993). The F/Cl ratios of the sediments along borehole ZK-01 are relatively high (up to 0.5 between 10 and 100 m) because the sediments may contain several metal oxides that can adsorb the F ions (e.g., Al, Fe), as indicated by the light red color (Vithanage and Bhattacharya 2015; Vithanage et al. 2012). In this study, most groundwater samples have high HCO_3^-/Ca ratios (Fig. 10e) with an alkaline

Fig. 12 Relationship between the apparent age (through ¹⁴C methods) and the fluoride concentration in some groundwater samples from Shihezi and Xiayedi oases



pH; this is a favorable geochemical condition for the dissolution of fluorite (Saxena and Ahmed 2003). The alkaline pH, larger than the point of zero charge of most minerals, could lead to the solid surface having negative charge and resisting the F adsorption processes, and thus promote F desorption when fluorine minerals react with the groundwater (Kumar et al. 2009; Sujana et al. 2009). Most groundwaters are undersaturated with fluorite, according to the negative fluorite saturation indices (Fig. 11), suggesting that the groundwater allows for the dissolution of additional fluorite; therefore, F in pore water and groundwater is originally and primarily derived from the sediments owing to water–rock interactions.

The Ca concentration or Na/Ca ratio in groundwater is considered as one of the major mechanisms driving F ion migration in this arid inland basin with terrestrial sediments. This mechanism was demonstrated by Currell et al. (2011) through a sediment–solution experiment, because low Ca concentrations can facilitate the dissolution of fluorite, while high Ca concentrations can easily help reach the CaF₂ solubility point and cause fluorite precipitation in the aqueous phase (Guo et al. 2012). It shows that cation exchange between Na and Ca is critical for improving geochemical conditions for the dissolution of F-bearing minerals and F migration. Most of the extremely elevated F groundwater samples (>4 mg/L) with low Ca concentrations in this study and other similar studies (Guo et al. 2012; Nordstrom and Jenne 1977) demonstrate this fact owing to the low fluorite solubility. The cation exchange between Ca (or Mg) and Na (or potassium) can be evaluated by the two chloro-alkaline indices CAI 1 and CAI 2. When cation exchange processes occur between the dissolved Na in groundwater and the adsorbed Ca in sediments, the CAI 1 and CAI 2 both have positive values; when it occurs in reverse order, the indices are both negative.

$$CAI\ 1 = [Cl - (Na + K)] / Cl \tag{5}$$

$$CAI\ 2 = [Cl - (Na + K)] / (SO_4 + CO_3 + HCO_3 + NO_3) \tag{6}$$

Negative CAI 1 and CAI 2 values in most of the groundwater samples (Fig. 13) indicate that the sediments can adsorb Ca from the groundwater and release Na into the groundwater in the presence of HCO₃ (Schoeller 1965), enhancing CaF₂ dissolution. The increasing monovalent Na concentrations relative to the divalent Ca concentrations can further reduce the repulsive potential between the positive hydrous metal oxide surfaces and negative ions with the help of alkaline conditions, and thus promote F desorption following the counterion effects (Li et al. 2015; Scanlon et al. 2009). In this study, Na/Ca ratios are consistently high with elevated F concentrations in most groundwater from the piedmont to the alluvial–fluvial plain. The relationship between F concentrations and Na/Ca ratios is not strongly positive in shallow ($R^2 = 0.12$), middle ($R^2 = 0.15$), or deep wells ($R^2 = 0.13$; Fig. 10d); it indicates that the distribution and migration of F is partially influenced by the Na/Ca ratios in the groundwater. The low R^2 values could attribute to the heterogeneous fluorite distributions in the aquifers and/or mixing with other high F sources at different depths across the basin.

Evapotranspiration is another process that could increase F concentrations in shallow groundwater under such an extreme

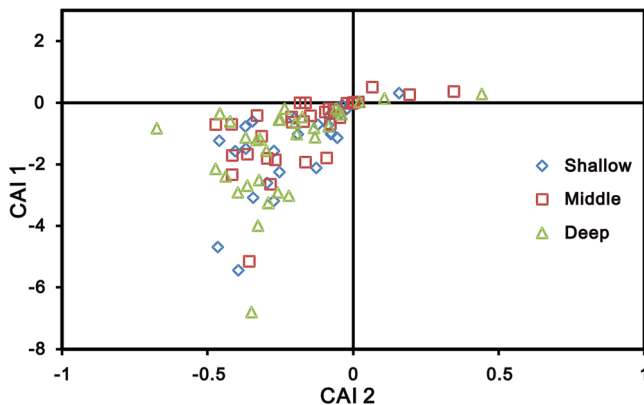


Fig. 13 Plot of chloro-alkaline indices CAI 2 vs CAI 1 for groundwater samples, indicating strong cation exchange between Na adsorbed onto the sediments and Ca into the groundwater, revealed from the negative values

arid climate. Two mechanisms are considered to explain the effects of evaporation on F enrichment. Intense evaporation and transpiration could concentrate the groundwater and increase the concentrations of all stable ions or reduced F/Cl and Na/Cl ratios; simultaneously, evaporation, but not transpiration, could cause the fractionation of hydrogen and oxygen isotopes. In some groundwater samples, positive relationships observed between $\delta^{18}\text{O}$ values and the Cl (Fig. 14a) and $\delta^{18}\text{O}$ values and F (Fig. 14b) concentrations indicate the evaporation effect. Evaporation also could cause the oversaturation of calcites and the prior precipitation can lower Ca concentrations and then promote the dissolution of fluorite as discussed already (Guo et al. 2007).

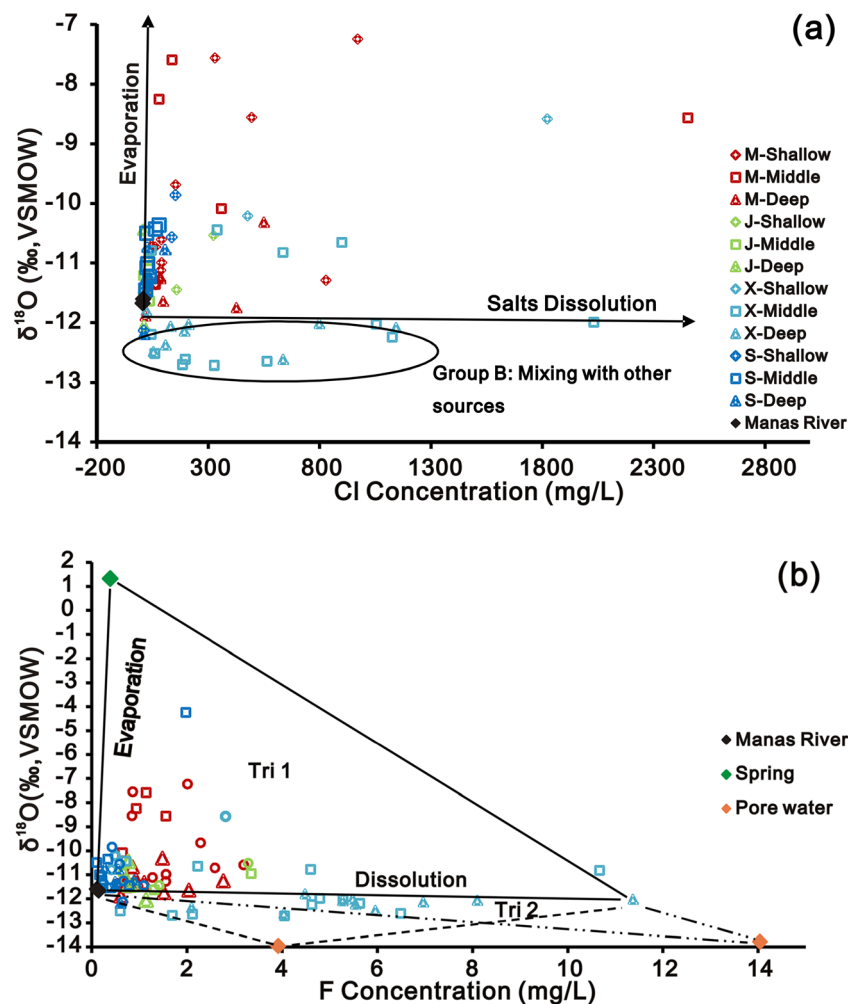
F ions in phreatic water can be transported, precipitate and accumulate in the vadose zone due to intense evaporation or transpiration effects. As reported in Table 4, high soluble F contents are distributed along the soil profiles (S1–S4) above the water table. As a result of the processes involved in agricultural activities, such as salt flushing and irrigation, soluble F contents in arable land can enter the groundwater during return flow (Han et al. 2011). Therefore, in addition to

water–rock interactions and evaporation, agricultural activities in oases may provide other sources of F and drive F migration through irrigation and the use of fertilizer and pesticides, as indicated by the elevated NO_3 in groundwater. The high NO_3 concentrations (>5 mg/L), with high F content in shallow, middle and deep wells (Fig. 10g), indicate that the agricultural activities affect the groundwater F migration in the MRB, mostly owing to fertilizer as well as animal and human wastes (Li et al. 2015). However, most groundwater samples with relatively high F concentrations (>4 mg/L) have low to medium NO_3 concentrations (0–14.1 mg/L). This indicates that input from agricultural activities affect the F enrichment only in the shallow and middle groundwater but do not act as a major source of F enrichment in the deep groundwater.

Influence of irrigation practices and groundwater exploitation

Groundwater from the deep aquifers has been exploited for flood irrigation and for flushing salt from the soil in the MRB for decades. This practice has made irrigation return flow and

Fig. 14 Plots of **a** $\delta^{18}\text{O}$ vs Cl and **b** $\delta^{18}\text{O}$ vs F concentration in groundwater, indicating that irrigation return flow and pore water in the aquitards contaminate groundwater, and leaching and vertical recharge are important processes for F mobilization and enrichment. M stands for Mosuowan, J for Jin'an, X for Xiayedi and S for Shihezi in the legend of part a



channel leakage important recharging sources of groundwater (Chen et al. 2009). The groundwater resources meet up to 50% of the total water demand, in particular for irrigation. Exploitation of the deep fresh groundwater causes reversal of the vertical hydraulic gradient between the shallow and deep aquifers. Shallow groundwater then can leak vertically into deep aquifers and contaminates the deep groundwater (Liu et al. 2015a).

The $\delta^{18}\text{O}$ and δD compositions of most groundwaters with high F concentrations are aligned with or slightly apart from the LMWL in Urumqi (Fig. 5). Low significance differences between F concentrations and major ion concentrations indicate that the groundwater mixes with other high-F sources, in addition to F being derived from geochemical processes. These high-F sources can be attributed to the local vertical recharge and mixing with the pore water in the aquitards (Mazor 2004; Xie et al. 2012). The vertical recharge, e.g. irrigation return flow and channel leakage, can also flush the salts, and simultaneously contribute to the groundwater hydrogeochemistry in this basin (Chen et al. 2009; Han et al. 2011; Ma et al. 2017). Slight increases in the Cl concentration with depleted $\delta^{18}\text{O}$ values in group B in Fig. 14a, i.e. mainly the middle and deep groundwater samples, indicate the presence of an additional recharge source in addition to the chemicals dissolution and evaporation that enrich the water with F (Li et al. 2015). Samples in group B have depleted $\delta^{18}\text{O}$ values to lower than those in Manas River and in the mountains, but with significant increases in Cl. This can likely be attributed to mixing with the paleo-water and to salts dissolution. In Fig. 14b, the F concentrations are plotted against the $\delta^{18}\text{O}$ values, and the groundwater samples occupy two triangular shapes (Tri 1 and Tri 2), identified by four end members: (1) the freshwater sample in the Manas River with low F concentration and low $\delta^{18}\text{O}$ value, considered as the original water (E_{Ori}); (2) a spring sample in the mountain area with enriched $\delta^{18}\text{O}$ and low F concentration, mainly the result of evaporation (E_{Eva}); (3) groundwater with extremely elevated F concentration and low $\delta^{18}\text{O}$ value ($E_{\text{HighF-gw}}$) and (4) pore water in the aquitards below 20 m with high F concentration and low $\delta^{18}\text{O}$ value (E_{Pore}). Most shallow and middle groundwater samples within Tri 1 present the combined effects of evaporation and fluorite dissolution. The nonlinearity in the relationship attributes to the mixing processes in the shallow and middle groundwater. Most of the extremely high F (>4 mg/L) samples are distributed in Tri 2, where the evaporation effects are neglected for isotopic signals and show no obvious evaporation effect. Pore water in the aquitards seems to affect the groundwater fluoride concentrations, particularly in the Xiayedi Oasis. The mixing processes of three of the end members are corroborated by the difference in the fluoride concentration and $\delta^{18}\text{O}$ value for the two groups of groundwater. Results of contribution ratios of the defined end members in the Tri 1 and Tri 2 groups are calculated by the linear

mixing model (Eqs. 7–9) and shown in Table 5. The generally small (mean value 9%) contribution of evaporation to the F concentrations in Tri 1 clearly indicates that the evaporated recharge, along with the products of fluorite dissolution, infiltrated quickly from the soil into the groundwater system (Datta et al. 1996), particularly the irrigation water from the Manas River with low F concentrations (0.13 mg/L). The contributions of pore water are underestimated because the lowest F concentration (3.92 mg/L) and $\delta^{18}\text{O}$ value (−13.97‰) along the ZK-01 profile are used. The mean contribution ratio, 21% (1–45%), indicates that the pore water in the aquitards affects the groundwater hydrochemistry in the aquifers and can increase the F concentration. Pore water in the aquitards is believed to preserve large amount of chemicals such as high F contents and depleted $\delta^{18}\text{O}$ isotopes. Aquitards prolong the migration residence time owing to their high porosity and low permeability, thereby increasing water–rock interactions under natural conditions (Hendry and Wassenar 2000, 2011; Hendry and Woodbury 2007). However, overexploitation of fresh groundwater can lead to groundwater cones of depression and the consolidation of aquitards. In depression-cone areas such as the Xiayedi Oasis, the observed inverse hydraulic gradient not only drives shallow groundwater leakage into the deep aquifer, facilitating the downward migration of the NO_3 -rich water from the shallow to the deep aquifers, but may also facilitate the release of pore water into aquifers during the consolidation processes of the aquitards (Ortega-Guerrero 2003; Ortega-Guerrero et al. 1993; Huang et al. 2012). Accordingly, the elevated-F groundwater evolves in three steps: (1) the fluorite in the soils are dissolved during the infiltration process (e.g. rainfall infiltration and irrigation return flow) into the shallow groundwater with an evaporation effect contribution ratio less than 40% in Tri 1 in Table 5; (2) dissolution of the fluorite occurs in the aquifers along the flow path and there is partial mixing with the existing elevated-F groundwater, e.g. water–rock interactions and leakage from the upper aquifers; (3) the groundwater is affected by the pore water in the aquitards (contribution ratios up to 45% in Tri 2 in Table 5). These results suggest that the Manas River and pumping groundwater for irrigation, at least to some degree, affect the F concentration distribution, migration and enrichment in groundwater.

The following Eqs. (7–9) express the mixing processes in Tri 1 and 2 (Fig. 14b) using the defined end members.

$$F_{\text{Ori}} + F_{\text{HighF-gw}} + F_{\text{Eva}} \cdot (F_{\text{Pore}}) = 1 \quad (7)$$

$$\begin{aligned} \text{Smp}(F) = & E_{\text{Ori}}(F) \cdot F_{\text{Ori}} + E_{\text{HighF-gw}}(F) \cdot F_{\text{HighF-gw}} \\ & + E_{\text{Eva}}(F) \cdot F_{\text{Eva}} \text{ (or } E_{\text{Pore}}(F) \cdot F_{\text{Pore}}) \end{aligned} \quad (8)$$

$$\begin{aligned} \text{Smp}({}^{18}\text{O}) = & E_{\text{Ori}}({}^{18}\text{O}) \cdot F_{\text{Ori}} + E_{\text{HighF-gw}}({}^{18}\text{O}) \cdot F_{\text{HighF-gw}} \\ & + E_{\text{Eva}}({}^{18}\text{O}) \cdot F_{\text{Eva}} \text{ (or } E_{\text{Pore}}({}^{18}\text{O}) \cdot F_{\text{Pore}}) \end{aligned} \quad (9)$$

Table 5 Contribution ratios of the F concentrations and $\delta^{18}\text{O}$ values in the mixing processes

	Tri 1 (62 samples, F = 1.16 mg/L)			Tri 2 (21 samples, F = 4.12 mg/L)		
	F_{Ori}	$F_{\text{HighF-gw}}$	F_{Eva}	F_{Ori}	$F_{\text{HighF-gw}}$	F_{Pore}
Mean	0.82	0.09	0.09	0.50	0.29	0.21
Max	0.99	0.40	0.57	0.88	0.68	0.45
Min	0.27	0.00	0.00	0.20	0.00	0.01
Median	0.88	0.06	0.05	0.46	0.38	0.18

The six samples do not locate in the triangular shapes and one is considered as the end member

where, F_{Ori} , $F_{\text{HighF-gw}}$, F_{Eva} and F_{Pore} are fractions of the original water, elevated-fluoride groundwater, evaporation, and pore water, respectively, and where E is the end member. $\text{Smp}(F)$ and $\text{Smp}(\delta^{18}\text{O})$ denote the fluoride concentration and $\delta^{18}\text{O}$ value for the sample, respectively.

Conceptual model of the fluoride migration in MRB

Pumping also disrupts the dynamic balance between the discharge and recharge processes, changes the groundwater flow paths, and redistributes F concentrations spatially. During the pumping process, the groundwater F is brought up to the surface and partially concentrated and accumulated in the vadose zone through soil sorption and evaporation-precipitation processes. Fresh irrigation return flow with low Ca concentrations (such as channel water for irrigation) promotes the dissolution of fluorite and drives the migration of concentrated F easily into the shallow and middle groundwater with the irrigation-elevated water table (Young et al. 2011). A certain amount of

fresh groundwater with extremely high F concentrations is distributed in the middle and deep wells in this study area. F concentrations are further increased in the vadose zone and shallow groundwater when fresh groundwater with an elevated F concentration is used as irrigation water (Datta et al. 1996). In summary, it is common that agricultural activities affect the F ion content of groundwater and F ion migration in Northwest China and the North China Plain, where groundwater with high F concentration is exploited to meet water requirements, and elevated F concentrations in pore water in the aquitards are observed (He et al. 2013; Li et al. 2015; Liu et al. 2015b; Kwong et al. 2015; Fig. 15). Thus, in the Xiayedi Oasis where the elevated-F groundwater is pumped for irrigation, the exploitation of elevated-F groundwater should be reduced and channels should be built to transport the Manas River water for irrigation using the popular mulched-drip irrigation method (Li et al. 2016), which could prevent the soil water from evaporation and reduce the amount of irrigation and return flow.

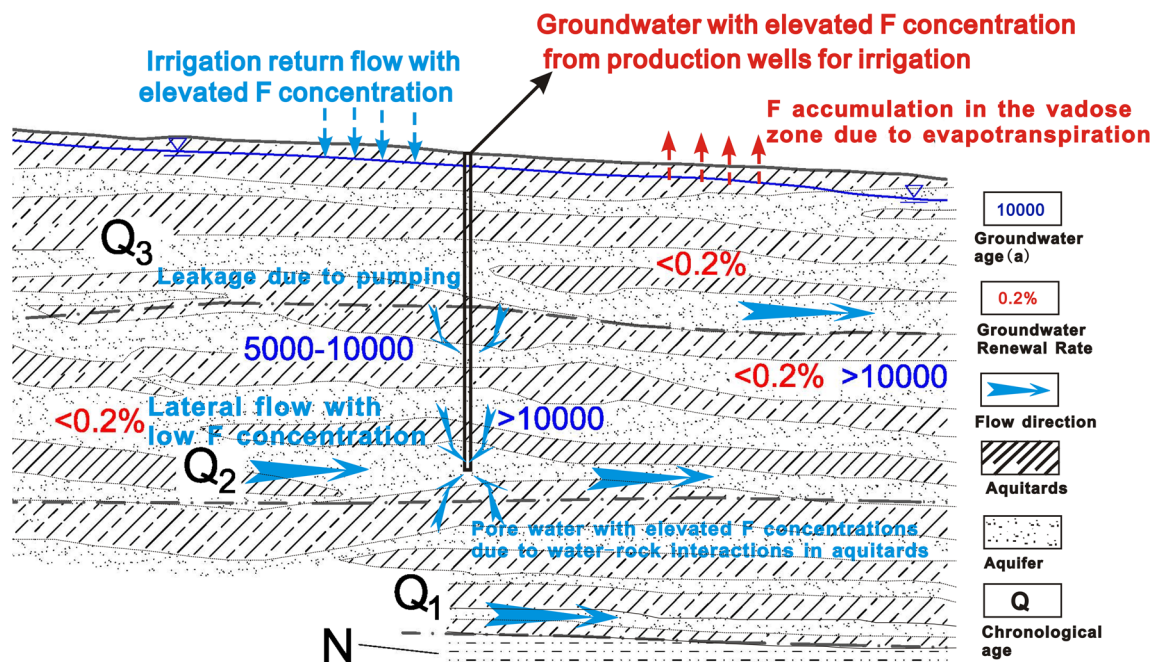


Fig. 15 A schematic diagram of fluoride migration driven by the agricultural activities in MRB (Q₃: Late Pleistocene, Q₂: Middle Pleistocene, Q₁: Early Pleistocene, N: Tertiary)

Conclusions

The F concentrations in the groundwater in the MRB generally increase along the flow path from the southeast piedmont to the northwest alluvial-fluvial plain, and groundwaters with elevated F concentration are mostly distributed in the arable land irrigated by groundwater. Particularly in the Xiayedi Oasis, F concentrations in the groundwater, soils, and pore water in the aquitards are higher than the concentration limit set by the WHO and generally show an increasing trend with increasing depth.

F ions in groundwater are mainly from the fluorite dissolution in sediments and accumulate through prolonged water–rock interactions and as a result of agricultural activities. The relationship between oxygen and hydrogen isotopes in the groundwater reveals a moderate evaporation effect on low-F groundwater. Elevated F concentrations coexist with high Na concentrations, low Ca concentrations, and high F/Cl and Na/Ca ratios under alkaline pH conditions. These indicate that the cation exchange processes between Na and Ca concentrations affect F migration and promote the dissolution of F-bearing minerals in the groundwater over a wide span of residence time. Meanwhile, the presence of high NO₃ in some elevated-F groundwater suggests that agricultural activities affect groundwater hydrogeochemistry and partially contribute to the migration and enrichment of F, particularly in shallow and middle aquifers. Wide variation in F and Cl concentrations along with slight differences in depleted $\delta^{18}\text{O}$ values demonstrate that leaching and mixing with vertical recharge could be the dominant hydrological processes that increase F concentrations.

Groundwater pumping not only disturbs the natural groundwater flow system and reverses hydraulic gradients but also increases the F content of the soils as well as shallow and middle groundwater due to the high F concentrations of the groundwater used for irrigation. Pore water with relatively high F concentrations in the aquitards is released into aquifers, resulting in an increase in F concentrations because of the aquitards consolidation due to the overexploitation of aquifer groundwater. This means that groundwater pumping for irrigation is responsible for F enrichment and migration and therefore must be strictly controlled in areas with high rates of endemic fluorine poisoning. This paper presents findings that have a common pattern and provides evidence to support the fact that both the extensive pumping of groundwater and irrigation control the enrichment and migration mechanisms of toxic ions such as F in Northwest China.

Acknowledgements The authors thank Professor Jinlong Zhou and Dr. Ruiliang Jia (Xinjiang Agricultural University) for providing field work assistance. We thank Dr. Jing Li for her constructive suggestions on this study.

Funding information This study was funded by the National Natural Science Foundation of China (Nos. U1403282 and 41672246) and the Fundamental Research Funds for the Central Universities, China University of Geosciences, Wuhan (CUGQYZX1712).

References

- Ali S, Thakur S, Sarkar A, Shekhar S (2016) Worldwide contamination of water by fluoride. *Environ Chem Lett* 14:291–315. <https://doi.org/10.1007/s10311-016-0563-5>
- Amini M, Mueller K, Abbaspour K, Rosenberg T, Afyuni M, Møller K, Sarr M, Johnson C (2008) Statistical modeling of global geogenic fluoride contamination in groundwaters. *Environ Sci Technol* 42:3662–3668. <https://doi.org/10.1021/es071958y>
- Ayoob S, Gupta AK (2006) Fluoride in drinking water: a review on the status and stress effects. *Crit Rev Environ Sci Technol* 36:433–487. <https://doi.org/10.1080/10643380600678112>
- Bothe O, Fraedrich K, Zhu X (2012) Precipitation climate of Central Asia and the large-scale atmospheric circulation. *Theor Appl Climatol* 108:345–354. <https://doi.org/10.1007/s00704-011-0537-2>
- Chae G-T, Yun S-T, Mayer B, Kim K-H, Kim S-Y, Kwon J-S, Kim K, Koh Y-K (2007) Fluorine geochemistry in bedrock groundwater of South Korea. *Sci Total Environ* 385:272–283. <https://doi.org/10.1016/j.scitotenv.2007.06.038>
- Chen TD, Chen XG, Wang WK et al (2009) Investigation and assessment of groundwater resources and its environmental issues in the Junggar Basin (in Chinese). Geological Publishing House, Peking, pp 25–79
- Currell M, Cartwright I, Raveggi M, Han D (2011) Controls on elevated fluoride and arsenic concentrations in groundwater from the Yuncheng Basin, China. *Appl Geochem* 26:540–552. <https://doi.org/10.1016/j.apgeochem.2011.01.012>
- Datta PS, Deb DL, Tyagi SK (1996) Stable isotope (¹⁸O) investigations on the processes controlling fluoride contamination of groundwater. *J Contam Hydrol* 24(1):85–96. [https://doi.org/10.1016/0169-7722\(96\)00004-6](https://doi.org/10.1016/0169-7722(96)00004-6)
- Gaciri SJ, Davies TC (1993) The occurrence and geochemistry of fluoride in some natural waters of Kenya. *J Hydrol* 143:395–412. [https://doi.org/10.1016/0022-1694\(93\)90201-J](https://doi.org/10.1016/0022-1694(93)90201-J)
- Guo Q, Wang Y, Ma T, Ma R (2007) Geochemical processes controlling the elevated fluoride concentrations in groundwaters of the Taiyuan Basin, northern China. *J Geochem Explor* 93:1–12. <https://doi.org/10.1016/j.gexplo.2006.07.001>
- Guo H, Zhang Y, Xing L, Jia Y (2012) Spatial variation in arsenic and fluoride concentrations of shallow groundwater from the town of Shihai in the Hetao basin, Inner Mongolia. *Appl Geochem* 27:2187–2196. <https://doi.org/10.1016/j.apgeochem.2012.01.016>
- Handa (1975) Geochemistry and genesis of fluoride-containing groundwaters in India. *Ground Water* 13:275–281. <https://doi.org/10.1111/j.1745-6584.1975.tb03086.x>
- Han D, Song X, Currell M, et al. (2011) A survey of groundwater levels and hydrogeochemistry in irrigated fields in the Karamay Agricultural Development Area, northwest China: Implications for soil and groundwater salinity resulting from surface water transfer for irrigation. *J Hydrol*, 405(3-4):217–234. <https://doi.org/10.1016/j.jhydrol.2011.03.052>
- He X, Ma T, Wang Y, Shan H, Deng Y (2013) Hydrogeochemistry of high fluoride groundwater in shallow aquifers, Hangjinhouqi, Hetao Plain. *J Geochem Explor* 135:63–70. <https://doi.org/10.1016/j.gexplo.2012.11.010>
- Hendry M, Wassenaar L (2000) Controls on the distribution of major ions in pore waters of a thick surficial aquitard. *Water Resour Res* 36:503–513. <https://doi.org/10.1029/1999WR900310>

- Hendry M, Wassenaar L (2011) Millennial-scale diffusive migration of solutes in thick clay-rich aquitards: evidence from multiple environmental tracers. *Hydrogeol J* 19:259–270. <https://doi.org/10.1007/s10040-010-0647-4>
- Hendry MJ, Woodbury AD (2007) Clay aquitards as archives of Holocene paleoclimate: $\delta^{18}\text{O}$ and thermal profiling. *Ground Water* 45:683–691. <https://doi.org/10.1111/j.1745-6584.2007.00354.x>
- Hendry MJ, Kelln CJ, Wassenaar LI, Shwa J (2004) Characterizing the hydrogeology of a complex clay-rich aquitard system using detailed vertical profiles of the stable isotopes of water. *J Hydrol* 293(1–4): 47–56. <https://doi.org/10.1016/j.jhydrol.2004.01.010>
- Huang Y, Scanlon BR, Nicot JP, Reedy RC, Dutton AR, Kelley VA, Deeds NE (2012) Sources of groundwater pumpage in a layered aquifer system in the Upper Gulf Coastal Plain, USA. *Hydrogeol J* 20:783–796. <https://doi.org/10.1007/s10040-012-0846-2>
- IAEA/WMO (2002) Global network of isotopes in precipitation. The GNIP database. IAEA, Vienna
- Irigoyen M, Molina N, Luengas I (1995) Prevalence and severity of dental fluorosis in a Mexican community with above-optimal fluoride concentration in drinking water. *Community Dent Oral* 23:243–245. <https://doi.org/10.1111/j.1600-0528.1995.tb00239.x>
- Jacks G, Bhattacharya P, Chaudhary V, Singh KP (2005) Controls on the genesis of some high-fluoride groundwaters in India. *Appl Geochem* 20:221–228. <https://doi.org/10.1016/j.apgeochem.2004.07.002>
- Kim Y, Kim J-Y, Kim K (2011) Geochemical characteristics of fluoride in groundwater of Gimcheon, Korea: lithogenic and agricultural origins. *Environ Earth Sci* 63:1139–1148. <https://doi.org/10.1007/s12665-010-0789-7>
- Kuang X, Jiao J, Wang Y (2016) Chloride as tracer of solute transport in the aquifer–aquitard system in the Pearl River Delta, China. *Hydrogeol J* 24:1121–1132. <https://doi.org/10.1007/s10040-016-1371-5>
- Kumar E, Bhatnagar A, Ji M, Jung W, Lee S-H, Kim S-J, Lee G, Song H, Choi J-Y, Yang J-S, Jeon B-H (2009) Defluoridation from aqueous solutions by granular ferric hydroxide (GFH). *Water Res* 43:490–498. <https://doi.org/10.1016/j.watres.2008.10.031>
- Kwong H, Jiao J (2016) Hydrochemical reactions and origin of offshore relatively fresh pore water from core samples in Hong Kong. *J Hydrol* 537:283–296. <https://doi.org/10.1016/j.jhydrol.2016.03.050>
- Kwong H, Jiao J, Liu K, Guo H, Yang S (2015) Geochemical signature of pore water from core samples and its implications on the origin of saline pore water in Cangzhou, North China Plain. *J Geochem Explor* 157:143–152. <https://doi.org/10.1016/j.gexplo.2015.06.008>
- Li J, Liang X, Jin M, Mao X (2013) Geochemical signature of aquitard pore water and its paleo-environment implications in Caofeidian Harbor, China. *Geochem J* 47:37–50. <https://doi.org/10.2343/geochemj.2.0238>
- Li C, Gao X, Wang Y (2015) Hydrogeochemistry of high-fluoride groundwater at Yuncheng Basin, northern China. *Sci Total Environ* 508:155–165. <https://doi.org/10.1016/j.scitotenv.2014.11.045>
- Li X, Jin M, Zhou N, Huang J, Jiang S, Telesphore H (2016) Evaluation of evapotranspiration and deep percolation under mulched drip irrigation in an oasis of Tarim basin, China. *J Hydrol* 538:677–688. <https://doi.org/10.1016/j.jhydrol.2016.04.045>
- Liu Z, Liu S, Chen D, Wang X (2006) Water resources composition and water circulation in plain of Manas River Basin (in Chinese with English Abstract). *J Hydraul Eng* 37(9):1102–1107
- Liu F, Song X, Yang L, Han D, Zhang Y, Ma Y, Bu H (2015a) The role of anthropogenic and natural factors in shaping the geochemical evolution of groundwater in the Subei Lake basin, Ordos energy base, northwestern China. *Sci Total Environ* 538:327–340. <https://doi.org/10.1016/j.scitotenv.2015.08.057>
- Liu H, Guo H, Yang L, Wu L, Li F, Li S, Ni P, Liang X (2015b) Occurrence and formation of high fluoride groundwater in the Hengshui area of the North China Plain. *Environ Earth Sci* 74(3): 2329–2340. <https://doi.org/10.1007/s12665-015-4225-x>
- Luan F, Zhou Y, Zhou J, Jia R, Zeng Y (2016) Distribution characteristics and enrichment factors of groundwater fluoride in Shihezi area of Xinjiang (in Chinese with English abstract). *Yellow River* 38(3):64–67
- Ma B, Jin M, Liang X, Li J (2017) Groundwater mixing and mineralization processes in a mountain–oasis–desert basin, Northwest China: hydrogeochemistry and environmental tracer indicators. *Hydrogeol J* 26(D22):1–18. <https://doi.org/10.1007/s10040-017-1659-0>
- Mazor E (2004) Chemical and isotopic groundwater hydrology. Dekker, New York
- Meenakshi, Garg VK, Kavita, Renuka, Malik A (2004) Groundwater quality in some villages of Haryana, India: focus on fluoride and fluorosis. *J Hazard Mater* 106:85–97. <https://doi.org/10.1016/j.jhazmat.2003.09.007>
- Ministry of Health of China (2015) China health statistical yearbook. Peking Union Medical College Press, Beijing
- Misra A, Mishra A (2007) Study of quaternary aquifers in Ganga Plain, India: focus on groundwater salinity, fluoride and fluorosis. *J Hazard Mater* 144:438–448. <https://doi.org/10.1016/j.jhazmat.2006.10.057>
- Negrel P, Pauwels H, Dewandel B, Gandolfi JM, Mascré C, Ahmed S (2011) Understanding groundwater systems and their functioning through the study of stable water isotopes in a hard-rock aquifer (Maheshwaram watershed, India). *J Hydrol* 397:55–70. <https://doi.org/10.1016/j.jhydrol.2010.11.033>
- Nordstrom D, Jenne E (1977) Fluorite solubility equilibria in selected geothermal waters. *Geochim Cosmochim Acta* 41:175–188. [https://doi.org/10.1016/0016-7037\(77\)90224-1](https://doi.org/10.1016/0016-7037(77)90224-1)
- Ortega-Guerrero A (2003) Origin and geochemical evolution of groundwater in a closed-basin clayey aquitard, northern Mexico. *J Hydrol* 284:26–44. [https://doi.org/10.1016/S0022-1694\(03\)00239-7](https://doi.org/10.1016/S0022-1694(03)00239-7)
- Ortega-Guerrero A, Cherry J, Rudolph D (1993) Large-scale aquitard consolidation near Mexico City. *Ground Water* 31:708–718. <https://doi.org/10.1111/j.1745-6584.1993.tb00841.x>
- Pang Z, Kong Y, Li J, Tian J (2017) An isotopic geoinicator in the hydrological cycle. *Procedia Earth Planet Sci* 17:534–537. <https://doi.org/10.1016/j.proeps.2016.12.135>
- Perrin J, Mascré C, Pauwels H, Ahmed S (2011) Solute recycling: an emerging threat to groundwater quality in southern India? *J Hydrol* 398:144–154. <https://doi.org/10.1016/j.jhydrol.2010.12.024>
- Rafique T, Naseem S, Usmani T, Bashir E, Khan F, Bhangar M (2009) Geochemical factors controlling the occurrence of high fluoride groundwater in the Nagar Parkar area, Sindh, Pakistan. *J Hazard Mater* 171:424–430. <https://doi.org/10.1016/j.jhazmat.2009.06.018>
- Rango T, Vengosh A, Jeuland M, Tekle-Haimanot R, Weinthal E, Kravchenko J, Paul C, McCormick P (2014) Fluoride exposure from groundwater as reflected by urinary fluoride and children's dental fluorosis in the Main Ethiopian Rift Valley. *Sci Total Environ* 496(496C):188–197. <https://doi.org/10.1016/j.scitotenv.2014.07.048>
- Rao N (2003) Groundwater quality: focus on fluoride concentration in rural parts of Guntur district, Andhra Pradesh, India. *Hydrol Sci J* 48:835–847. <https://doi.org/10.1623/hysj.48.5.835.51449>
- Reddy DV, Nagabhusanam P, Sukhija BS, Reddy AGS, Smedley PL (2010) Fluoride dynamics in the granitic aquifer of the Wailapally watershed, Nalgonda District, India. *Chem Geol* 269:278–289. <https://doi.org/10.1016/j.chemgeo.2009.10.003>
- Rockström J, Falkenmark M, Karlberg L, Hoff H, Rost S, Gerten D (2009) Future water availability for global food production: the potential of green water for increasing resilience to global change. *Water Resour Res* 45. <https://doi.org/10.1029/2007WR006767>
- Saether OM, Andreassen BT, Semb A (1995) Amounts and sources of fluoride in precipitation over southern Norway. *Atmos Environ* 29: 1785–1793. [https://doi.org/10.1016/1352-2310\(95\)00100-D](https://doi.org/10.1016/1352-2310(95)00100-D)

- Salle CLGL, Marlin C, Leduc C, Taupin JD, Massault M, Favreau G (2001) Renewal rate estimation of groundwater based on radioactive tracers (^3H , ^{14}C) in an unconfined aquifer in a semi-arid area, Iullemeden basin, Niger. *J Hydrol* 254(1):145–156
- Saxena V, Ahmed S (2003) Inferring the chemical parameters for the dissolution of fluoride in groundwater. *Environ Geol* 43(6):731–736. <https://doi.org/10.1007/s00254-002-0672-2>
- Scanlon BR, Nicot JP, Reedy RC, Kurtzman D, Mukherjee A, Nordstrom DK (2009) Elevated naturally occurring arsenic in a semiarid oxidizing system, Southern High Plains aquifer, Texas, USA. *Appl Geochem* 24:2061–2071. <https://doi.org/10.1016/j.apgeochem.2009.08.004>
- Schoeller H (1965) Qualitative evaluation of groundwater resources: methods and techniques of groundwater investigations and development. UNESCO, Paris, pp 54–83
- Su C, Wang Y, Xie X, Zhu Y (2015) An isotope hydrochemical approach to understand fluoride release into groundwaters of the Datong Basin, northern China. *Environ Sci Processes Impacts* 17(4):791–801. <https://doi.org/10.1039/C4EM00584H>
- Sujana MG, Pradhan HK, Anand S (2009) Studies on sorption of some geomaterials for fluoride removal from aqueous solutions. *J Hazard Mater* 161:120–125. <https://doi.org/10.1016/j.jhazmat.2008.03.062>
- Tekle-Haimanot R, Melaku Z, Kloos H, Reimann C, Fantaye W, Zerihun L, Bjorvatn K (2006) The geographic distribution of fluoride in surface and groundwater in Ethiopia with an emphasis on the Rift Valley. *Sci Total Environ* 367:182–190. <https://doi.org/10.1016/j.scitotenv.2005.11.003>
- Tian H, Wang WK, Jing XY, Deng L (2010) A study on tritium of groundwater in Manas River basin (in Chinese with English abstract). *J Arid Land Res Environ* 24(3):98–102
- Vikas C, Kushwaha R, Ahmad W, Prasannakumar V, Reghunath R (2013) Genesis and geochemistry of high fluoride bearing groundwater from a semi-arid terrain of NW India. *Environ Earth Sci* 68:289–305. <https://doi.org/10.1007/s12665-012-1739-3>
- Vithanage M, Bhattacharya P (2015) Fluoride in the environment: sources, distribution and defluoridation. *Environ Chem Lett* 13:131–147. <https://doi.org/10.1007/s10311-015-0496-4>
- Vithanage M, Jayarathna L, Rajapaksha A, Dissanayake CB, Bootharaju MS, Pradeep T (2012) Modeling sorption of fluoride on to iron rich laterite. *Colloids Surface A* 398:69–75. <https://doi.org/10.1016/j.colsurfa.2012.02.011>
- Wang S, Zhang M, Che Y, Chen F, Qiang F (2016) Contribution of recycled moisture to precipitation in oases of arid Central Asia: a stable isotope approach. *Water Resour Res* 52:3246–3257. <https://doi.org/10.1002/2015WR018135>
- Wenzel WW, Blum WE (1992) Fluorine speciation and mobility in F-contaminated soils. *Soil Sci* 153:357–364. <https://doi.org/10.1097/00010694-199205000-00003>
- WHO (2004) Fluoride in drinking water-background document for development of WHO guidelines for drinking water quality. WHO, Geneva
- Williams WD (1999) Salinisation: a major threat to water resources in the arid and semi-arid regions of the world. *Lakes Reserv Res Manag* 4:85–91. <https://doi.org/10.1046/j.1440-1770.1999.00089.x>
- Xie X, Wang Y, Su C, Li J, Li M (2012) Influence of irrigation practices on arsenic mobilization: evidence from isotope composition and Cl/Br ratios in groundwater from Datong Basin, northern China. *J Hydrol* 424–425:3747. <https://doi.org/10.1016/j.jhydrol.2011.12.017>
- Young SM, Pitawala A, Ishiga H (2011) Factors controlling fluoride contents of groundwater in north-central and northwestern Sri Lanka. *Environ Earth Sci* 63(6):1333–1342. <https://doi.org/10.1007/s12665-010-0804-z>
- Zhou Z, Guo Q, Dou Z (2013) Delayed drainage of aquitard in response to sudden change in groundwater level in adjacent confined aquifer: analytical and experimental studies. *Chin Sci Bull* 58:3060–3069. <https://doi.org/10.1007/s11434-013-5730-5>